Uncertainties in Low-energy Neutrino-nucleus Scattering

Vishvas Pandey

Fermi National Accelerator Laboratory

Theoretical Physics Uncertainties to Empower Neutrino Experiments, INT Seattle, October 30 - November 3, 2023

Low-energy Neutrino-nucleus Scattering

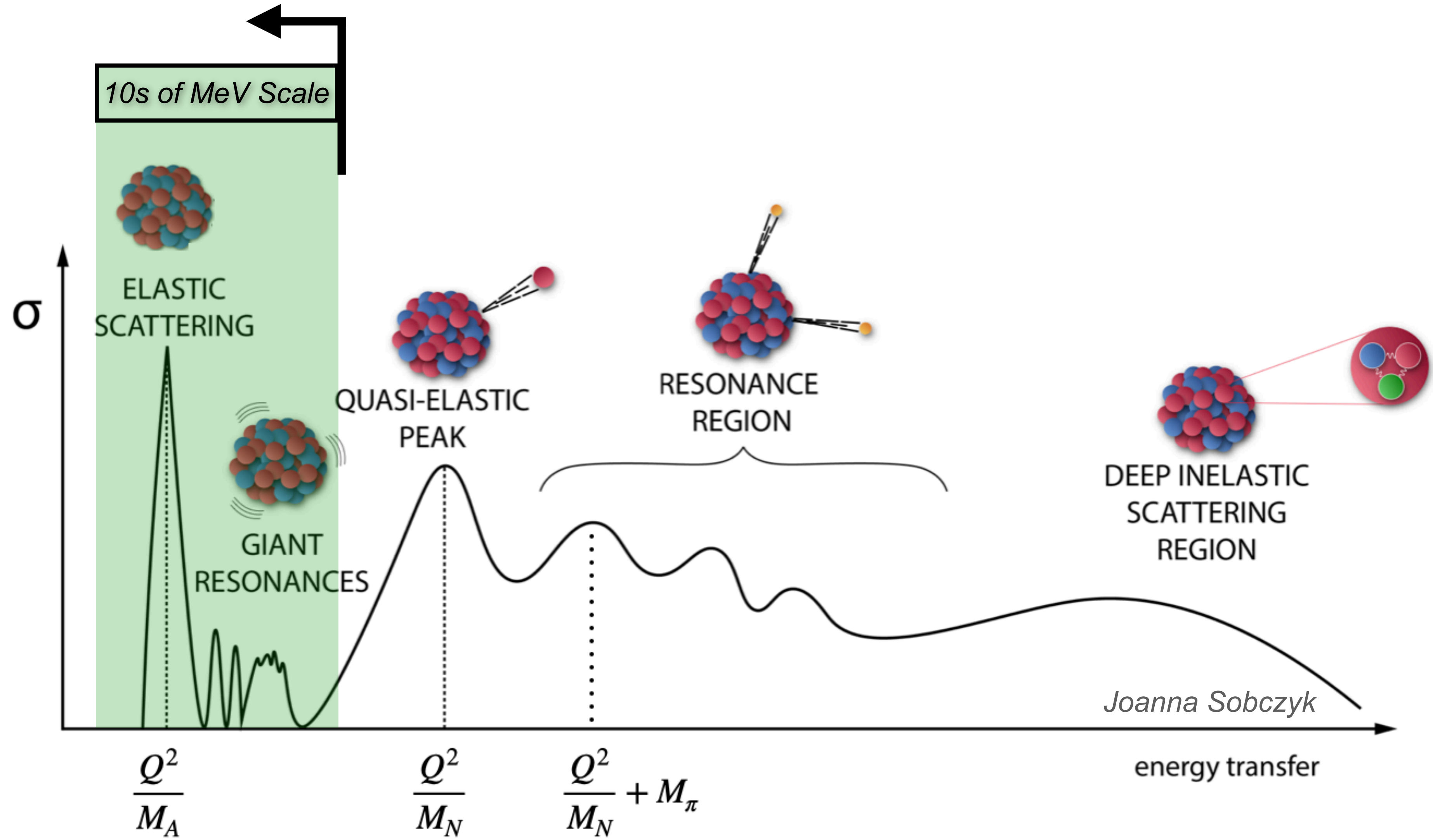

Low-energy Neutrino-nucleus Scattering

Coherent elastic [CEvNS]

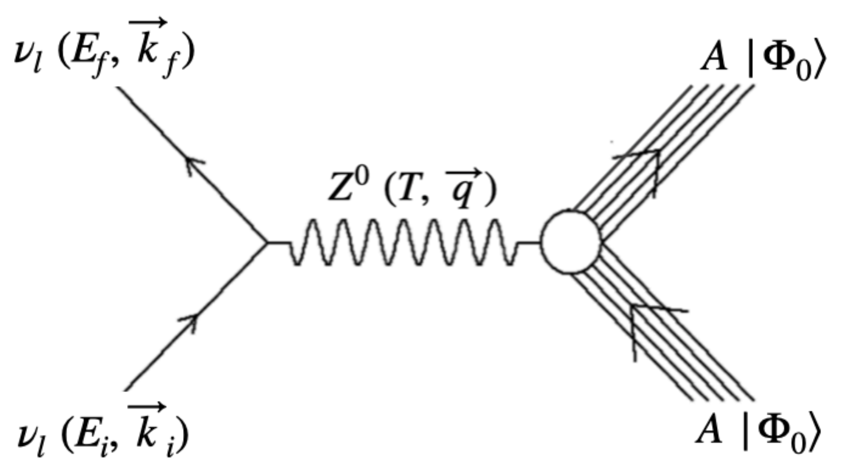

Inelastic CC/NC

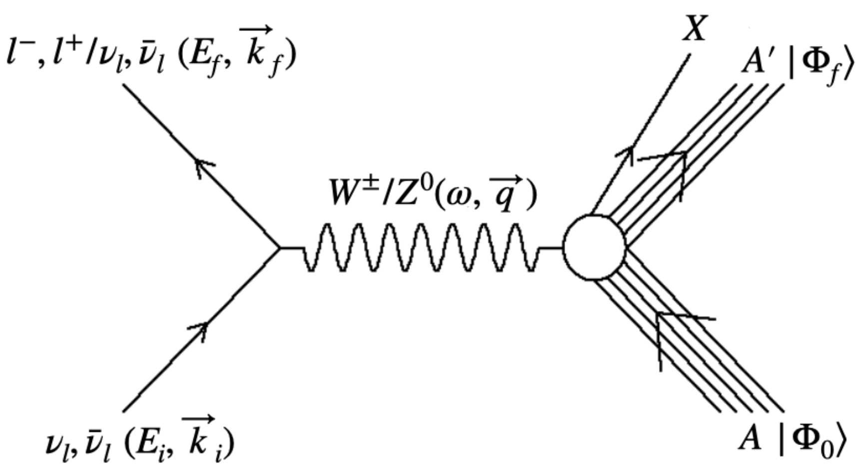

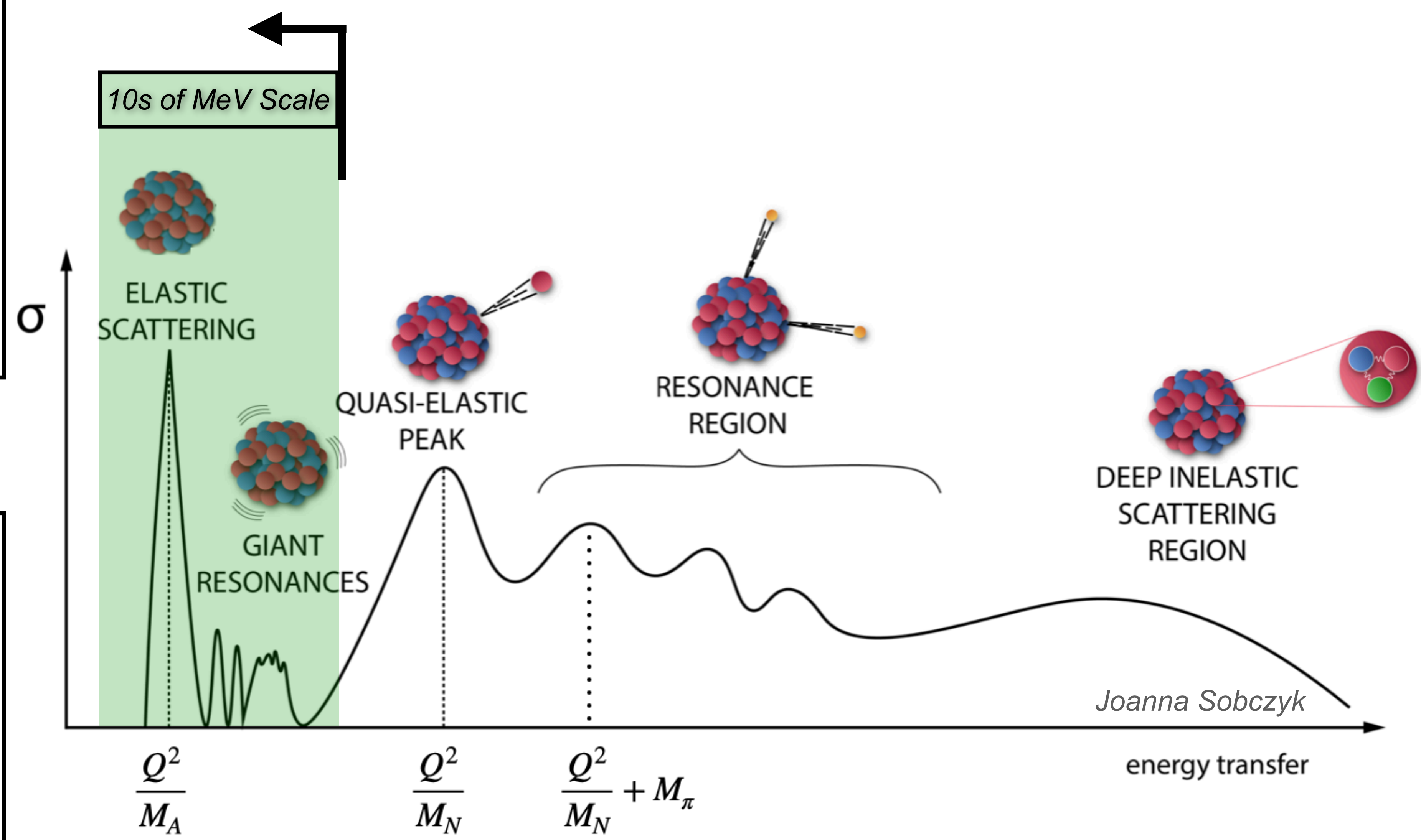

Low-energy Neutrino-nucleus Scattering

- V. Pandey, Prog. Part. Nucl. Phys., 104078 (2023)
  "Recent Progress in Low Energy Neutrino Scattering Physics and Its Implications for the Standard and Beyond the Standard Model Physics"

- N. Van Dessel, V. Pandey, H. Ray and N. Jachowicz, Universe 9, 207 (2023)
  "Cross Sections for Coherent Elastic and Inelastic Neutrino-Nucleus Scattering"

- B. Dutta, W. C. Huang, J. L. Newstead and V. Pandey, Phys. Rev. D 106, 113006 (2022)
  "Inelastic nuclear scattering from neutrinos and dark matter"

- O. Tomalak, P. Machado, V. Pandey and R. Plestid, JHEP 02, 097 (2021)
  "Flavor-dependent radiative corrections in coherent elastic neutrino-nucleus scattering"

Low-energy Neutrino-nucleus Scattering

- V. Pandey, Prog. Part. Nucl. Phys., 104078 (2023)
  "Recent Progress in Low Energy Neutrino Scattering Physics and Its Implications for the Standard and Beyond the Standard Model Physics"

- N. Van Dessel, V. Pandey, H. Ray and N. Jachowicz, Universe 9, 207 (2023)
  "Cross Sections for Coherent Elastic and Inelastic Neutrino-Nucleus Scattering"

- B. Dutta, W. C. Huang, J. L. Newstead and V. Pandey, Phys. Rev. D 106, 113006 (2022)
  "Inelastic nuclear scattering from neutrinos and dark matter"

- O. Tomalak, P. Machado, V. Pandey and R. Plestid, JHEP 02, 097 (2021)
  "Flavor-dependent radiative corrections in coherent elastic neutrino-nucleus scattering"

- INT Workshop (23-85), April 2023

APRIL 17 - APRIL 21, 2023
Interplay of Nuclear, Neutrino and BSM Physics at Low-Energies (23-85W)
Bhaskar Dutta, Jayden Newstead, Vishvas Pandey

- MITP Workshop, June 2023

Neutrino Scattering at Low and Intermediate Energies
June 26 – 30, 2023
Joanna Sobczyk, Adi Ashkenazi, Steven Gardiner

✦ $E_\nu \approx$ 10s of MeV

- **Pion decay-at-rest neutrinos**
  (SNS at ORNL, LANSCE at LANL, MLF at JPARC, FNAL, …)

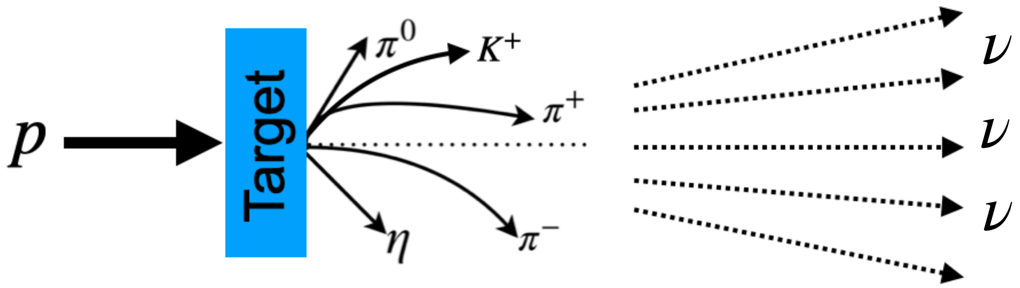

- **Core-collapse Supernova Neutrinos**

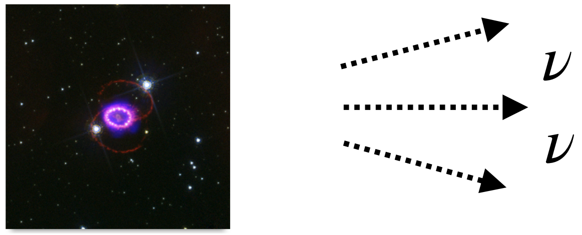

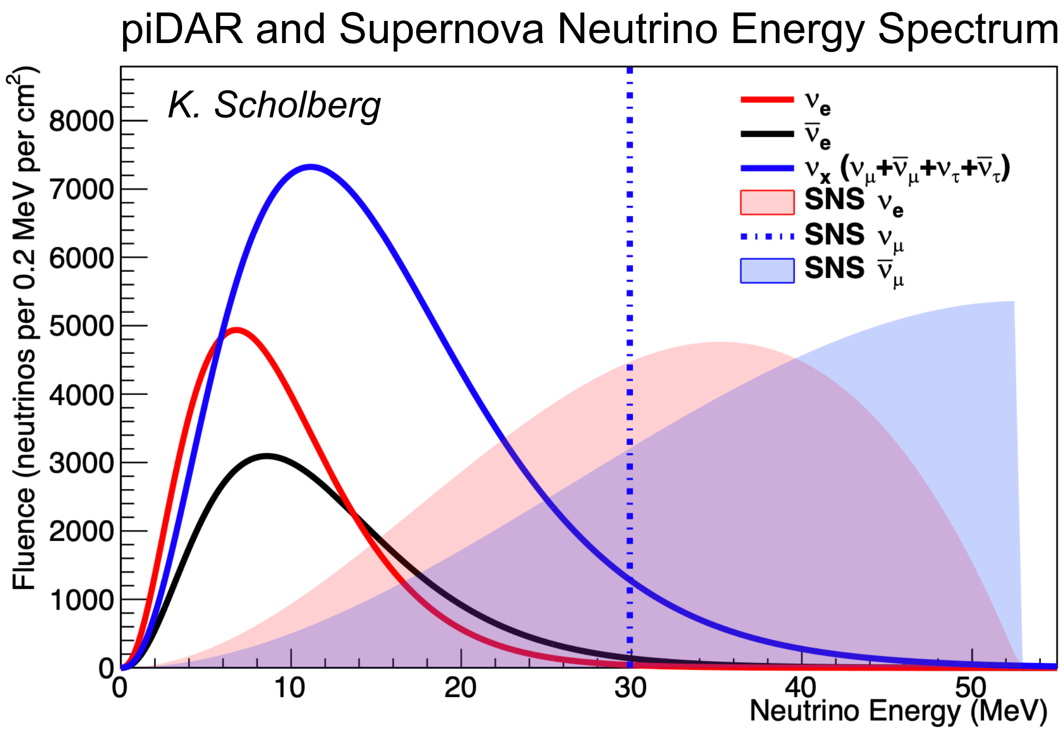

Neutrino Sources and Physics Scope

✦ $E_\nu \approx$ 10s of MeV

- **Pion decay-at-rest neutrinos**
  (SNS at ORNL, LANSCE at LANL, MLF at JPARC, FNAL, …)

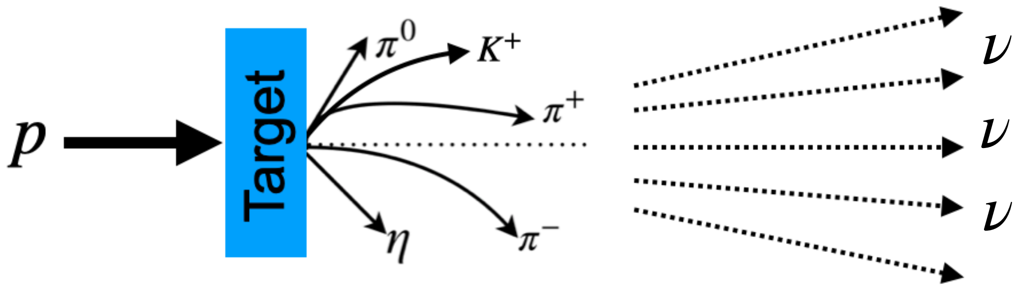

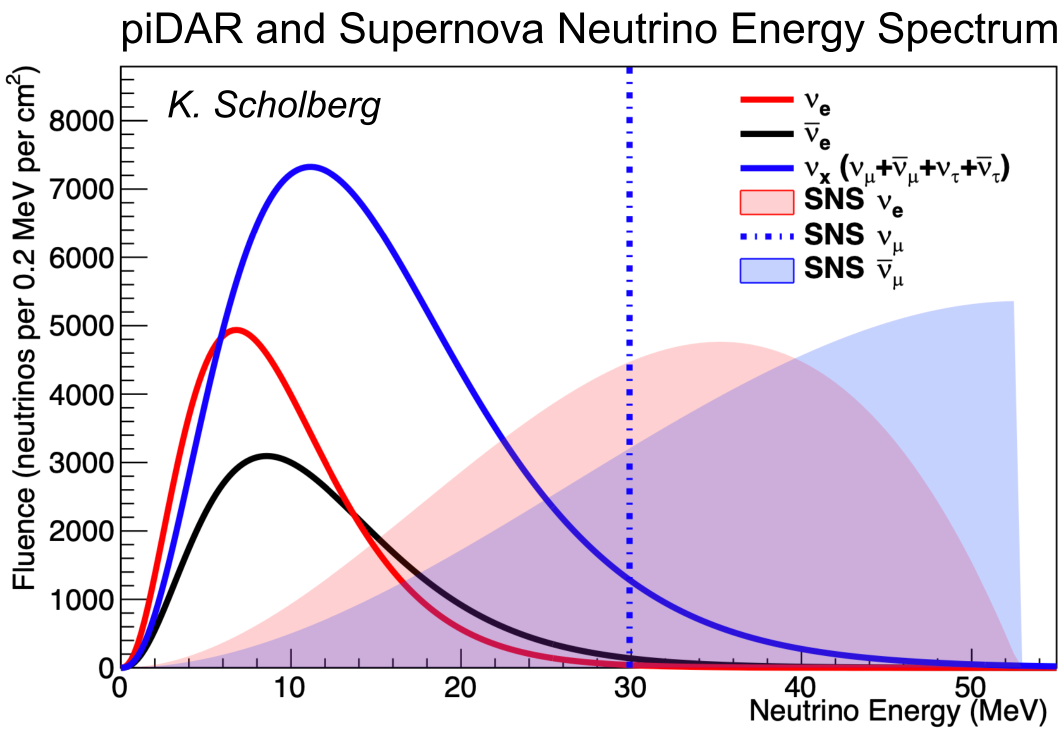

- **Core-collapse Supernova Neutrinos**

✦ 10s MeV scale physics in GeV scale ν beam

- **Pion decay-in-flight neutrinos**
  (BNB/NUMI/LBNF at FNAL, JPARC, …)

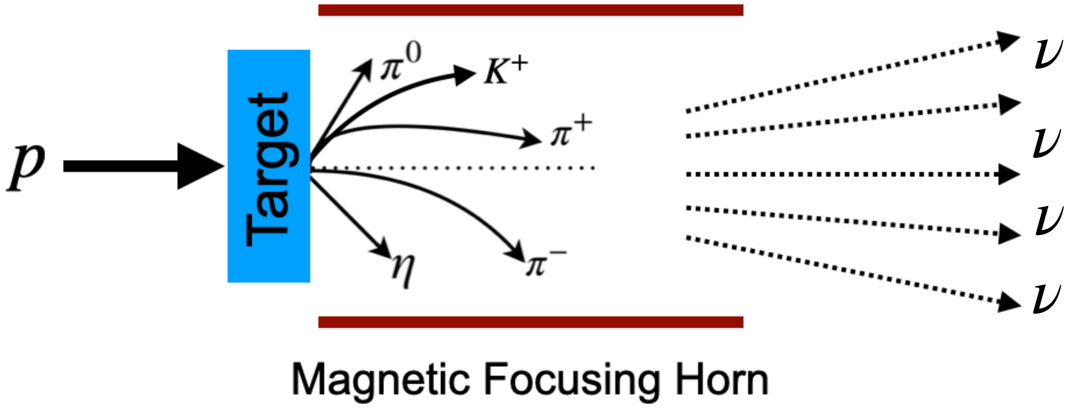

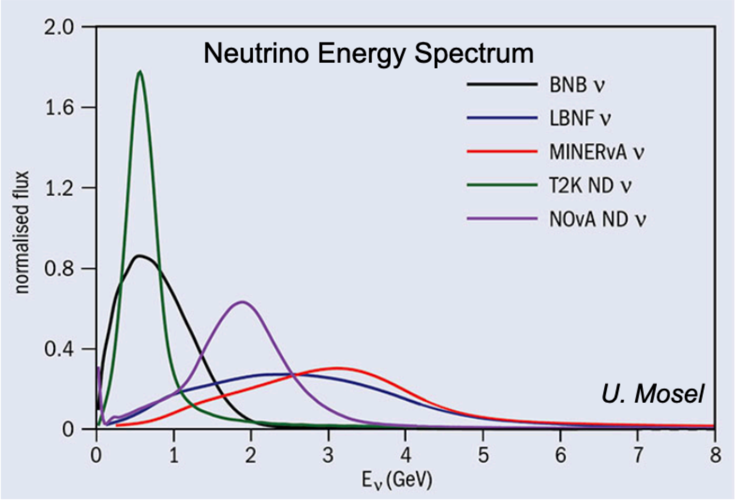

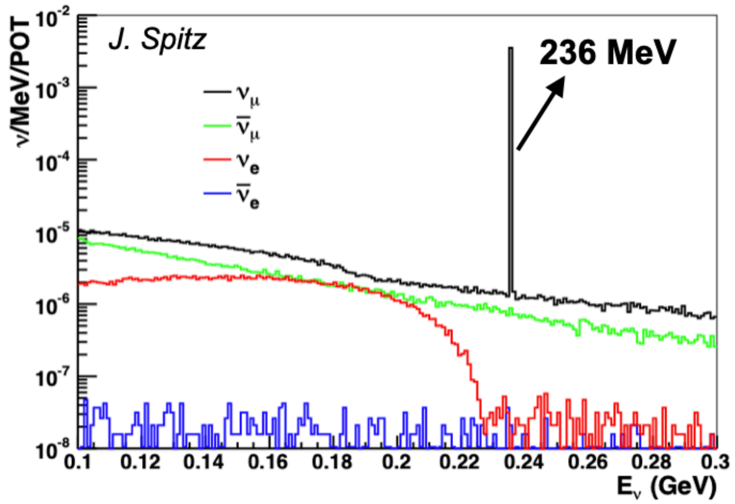

Fermilab

Neutrino Sources and Physics Scope

✦ $E_\nu \approx$ 10s of MeV

- **Pion decay-at-rest neutrinos**
  (SNS at ORNL, LANSCE at LANL, MLF at JPARC, FNAL, …)

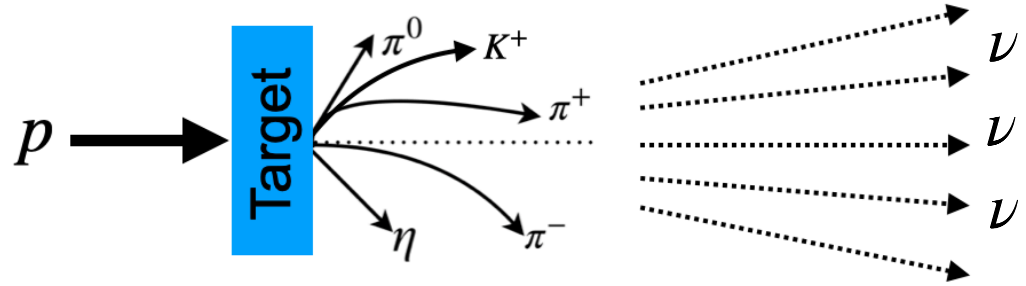

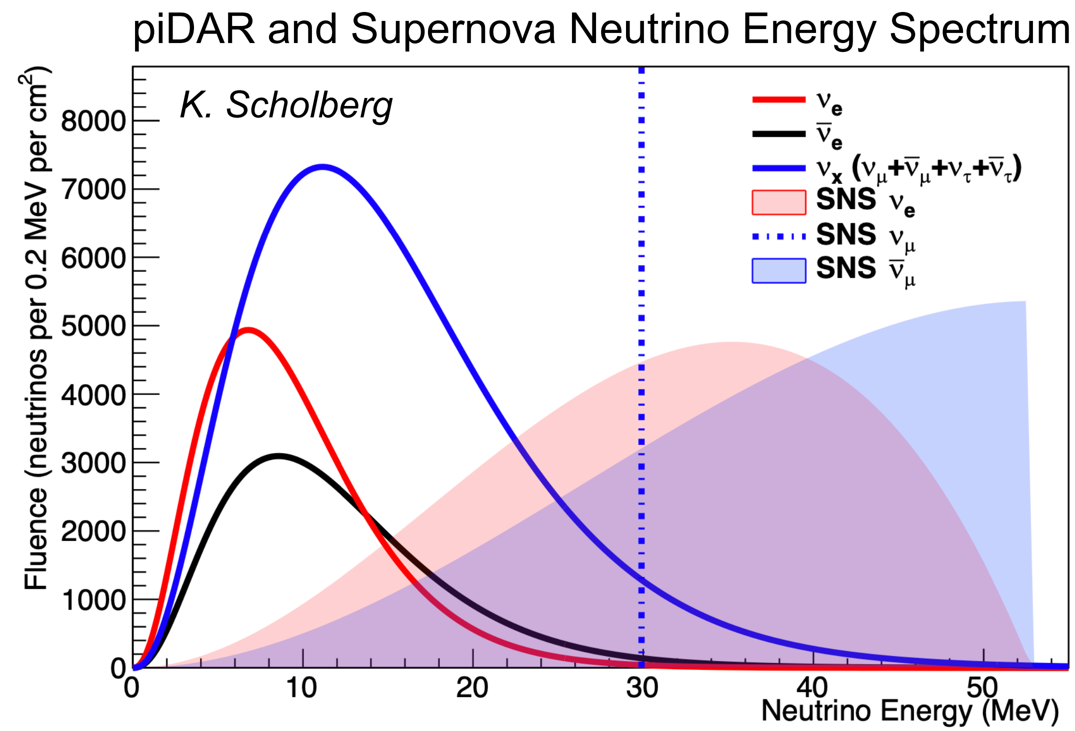

- **Core-collapse Supernova Neutrinos**

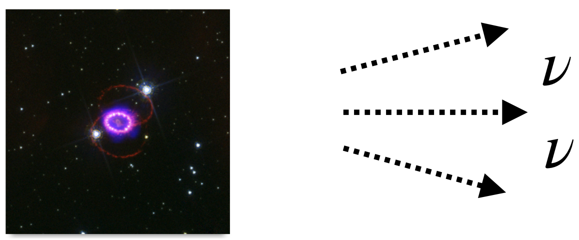

Neutrino physics, SM precision test, astrophysics, nuclear physics, BSM physics

✦ 10s MeV scale physics in GeV scale ν beam

- **Pion decay-in-flight neutrinos**
  (BNB/NUMI/LBNF at FNAL, JPARC, …)

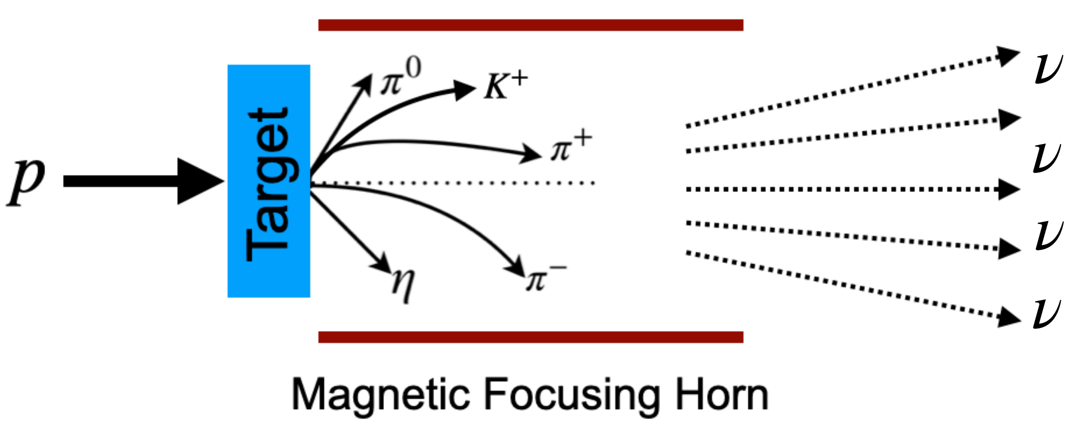

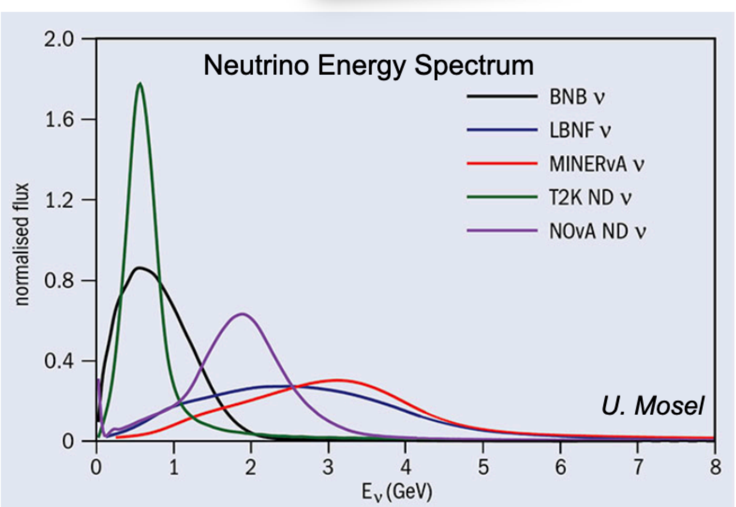

Kaon decay at rest

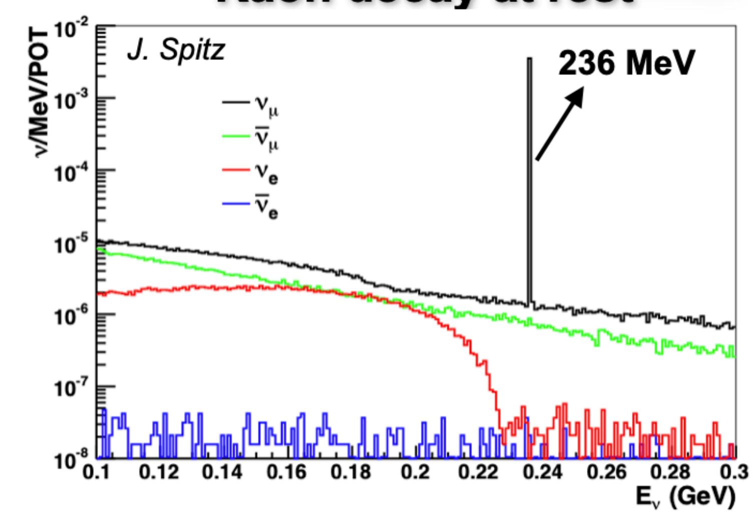

10s of MeV Neutrinos-Nucleus Scattering

Coherent elastic [CEvNS]

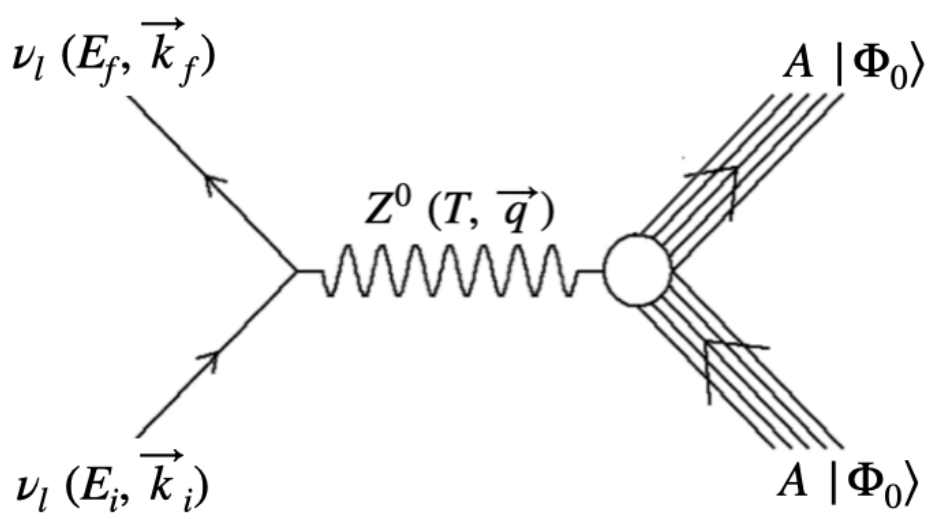

- Final state nucleus stays in its ground state
- Tiny recoil energy, large cross section
- Signal: keV energy nuclear recoil

Inelastic CC/NC

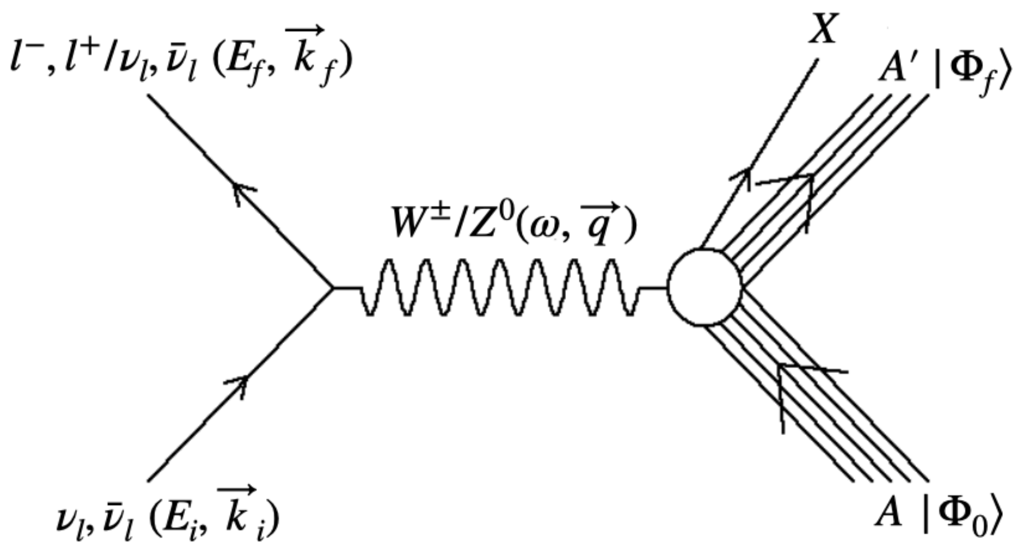

- Nucleus excites to states with well-defined excitation energy, spin and parity (J^π)
- Followed by nuclear de-excitation into MeV energy gammas, including n, p or nuclear fragmentation emission.

10s of MeV Neutrinos-Nucleus Scattering

Coherent elastic [CEvNS]

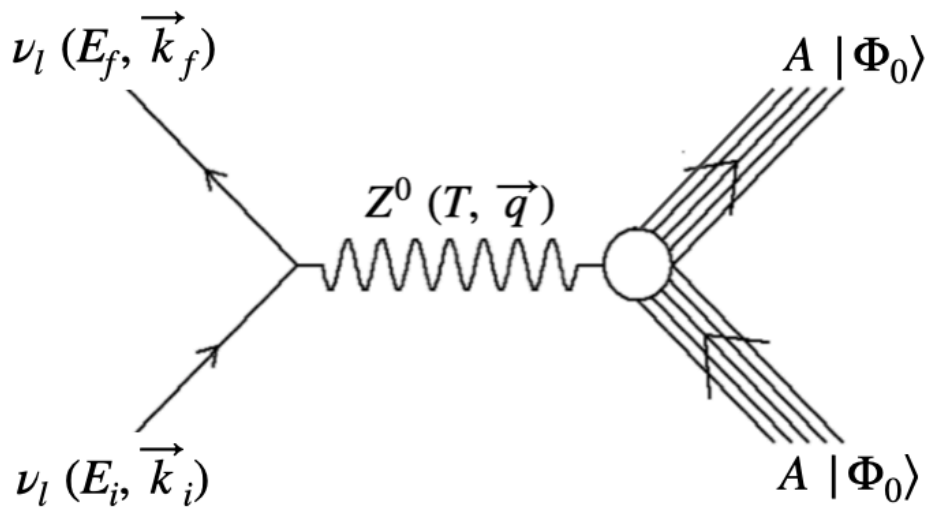

- Final state nucleus stays in its ground state
- Tiny recoil energy, large cross section
- Signal: keV energy nuclear recoil

Inelastic CC/NC

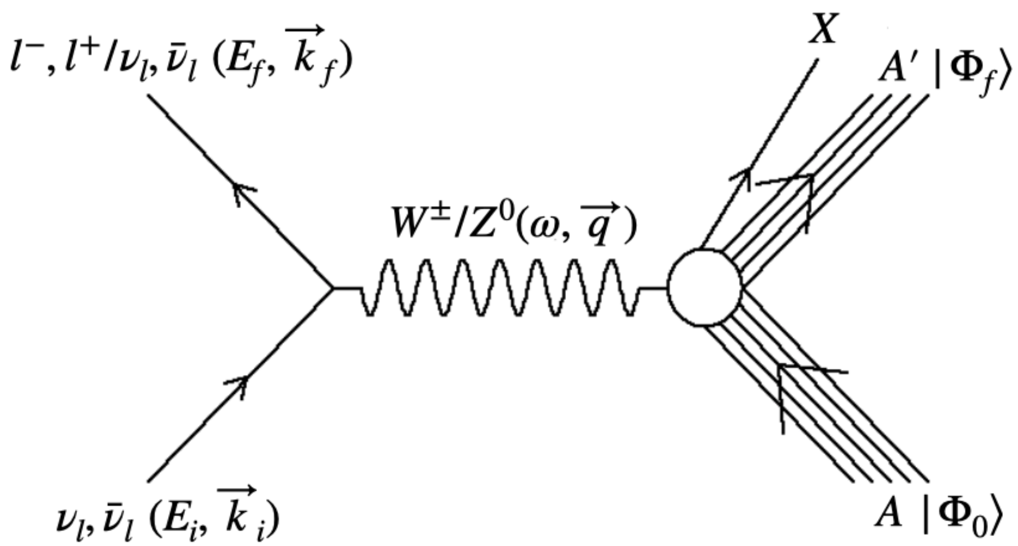

- Nucleus excites to states with well-defined excitation energy, spin and parity (J^π)
- Followed by nuclear de-excitation into MeV energy gammas, including n, p or nuclear fragmentation emission.

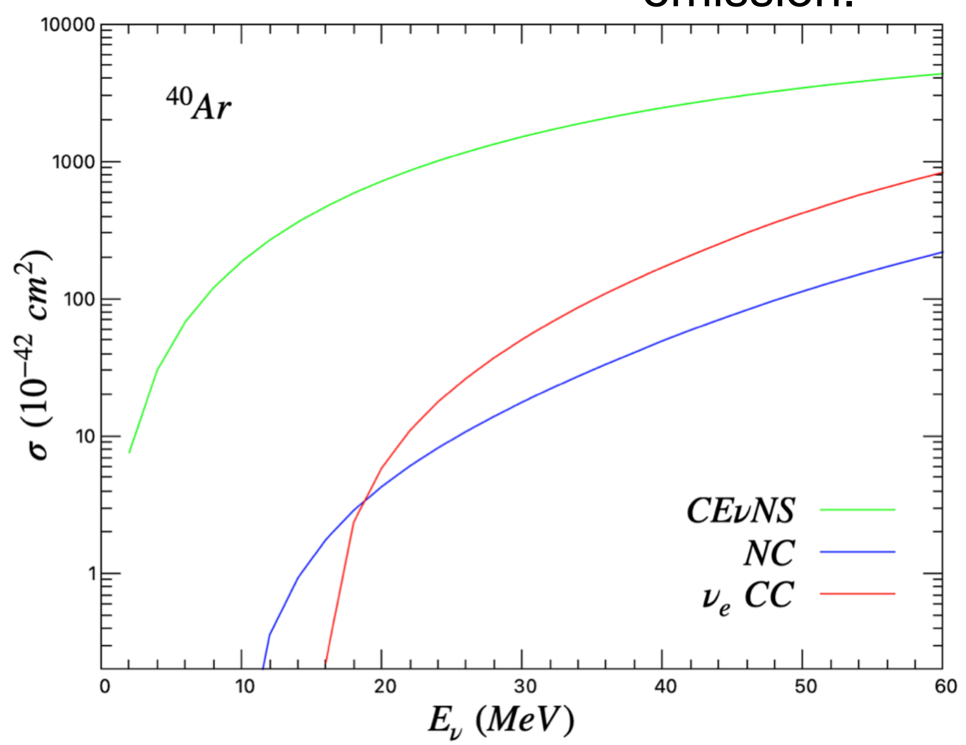

- At 10s of MeV, CEvNS cross section is significantly larger than inelastic ones.

10s of MeV Neutrinos-Nucleus Scattering

Coherent elastic [CEvNS]

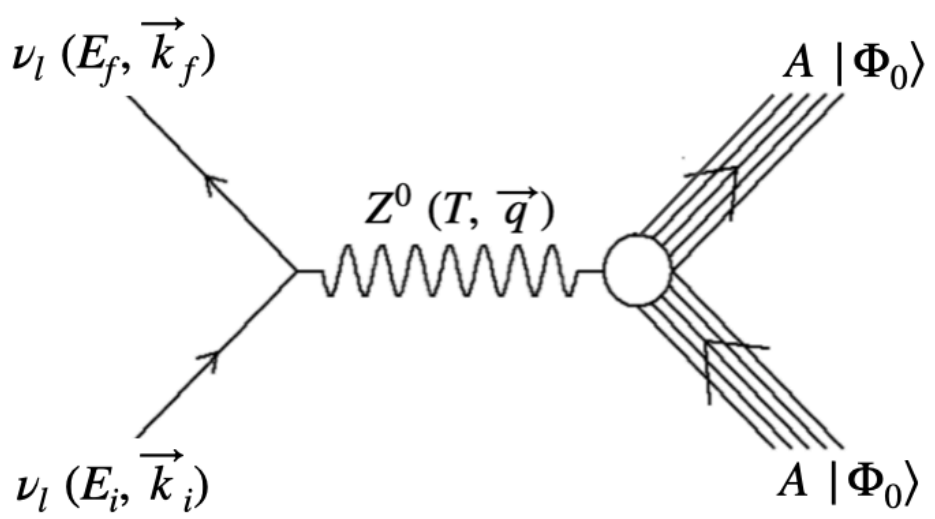

Inelastic CC/NC

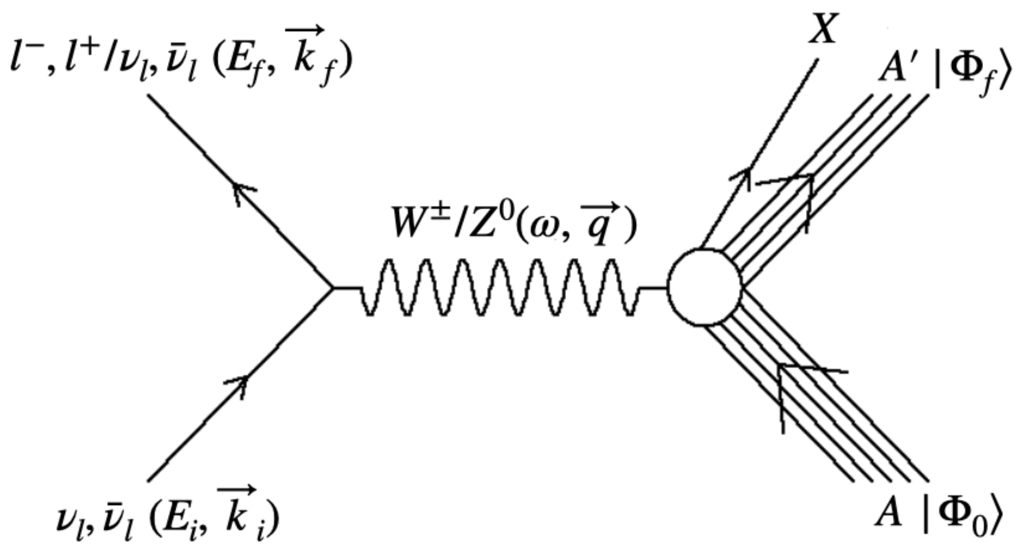

$$\sum_{fi} |\mathscr{M}|^2 \propto \frac{G_F^2}{2} L_{\mu\nu} W^{\mu\nu}$$

Leptonic Tensor: $L_{\mu\nu} = \sum_{fi} (\mathscr{J}_{l,\mu})^\dagger \mathscr{J}_{l,\nu}$ Hadronic Tensor: $W^{\mu\nu} = \sum_{fi} (\mathscr{J}_n^\mu)^\dagger \mathscr{J}_n^\nu$

Coherent elastic [CEvNS]

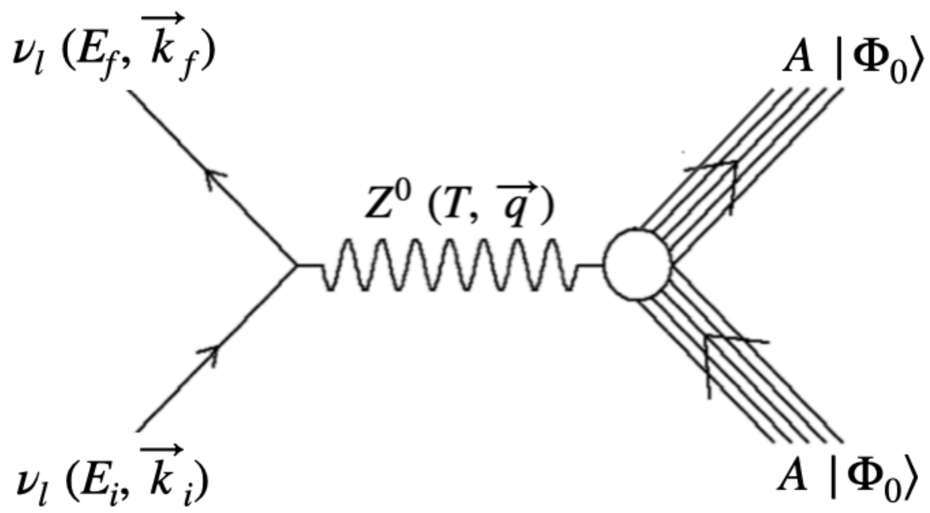

Inelastic CC/NC

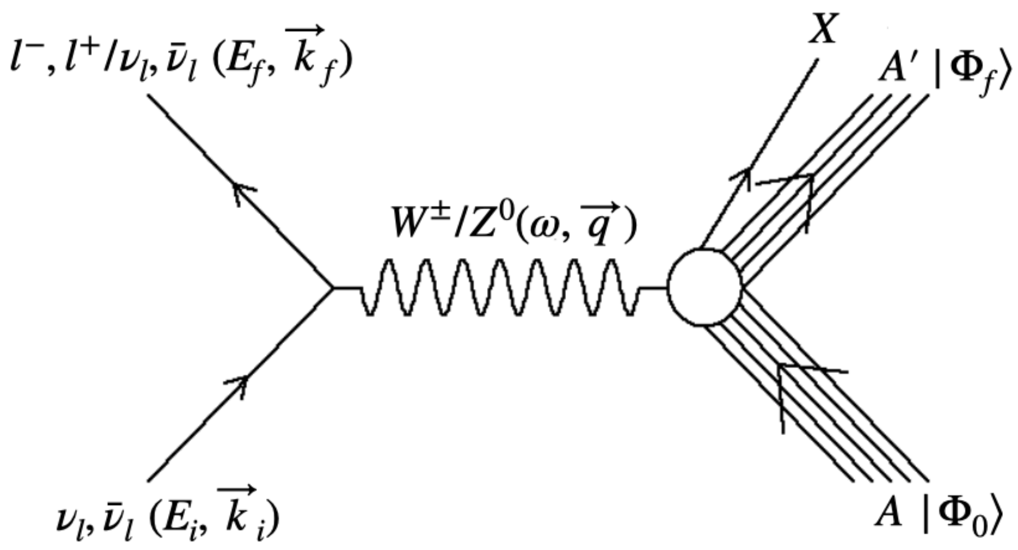

$$\sum_{fi} |\mathscr{M}|^2 \propto \frac{G_F^2}{2} L_{\mu\nu} W^{\mu\nu}$$

Leptonic Tensor: $L_{\mu\nu} = \sum_{fi} (\mathscr{J}_{l,\mu})^\dagger \mathscr{J}_{l,\nu}$ Hadronic Tensor: $W^{\mu\nu} = \sum_{fi} (\mathscr{J}_n^\mu)^\dagger \mathscr{J}_n^\nu$

Transition Amplitude: $\mathscr{J}_n^\mu = \langle \Phi_0 | \hat{J}_n^\mu(q) | \Phi_0 \rangle$

Cross Section:

$$d\sigma \propto \frac{G_F^2}{4\pi}\, Q_W^2 F_W^2(q)$$

10s of MeV Neutrinos-Nucleus Scattering

Coherent elastic [CEvNS]

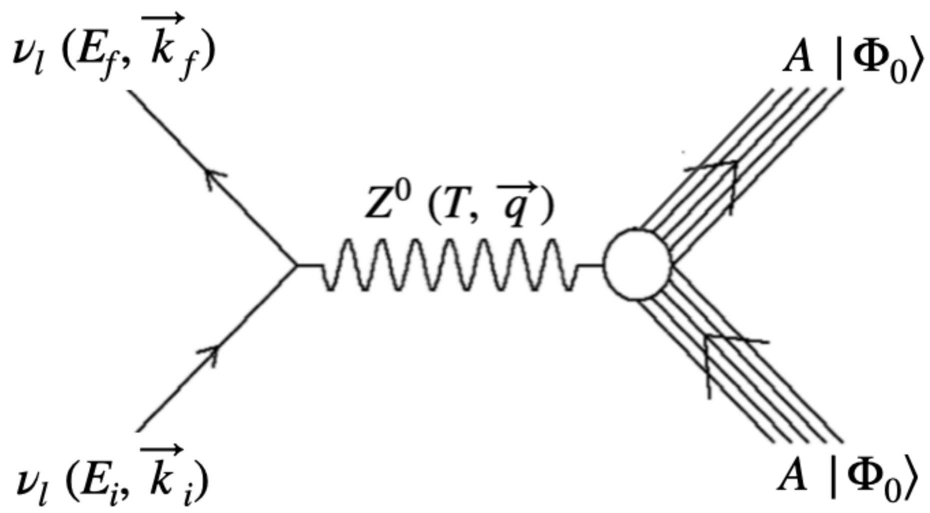

Inelastic CC/NC

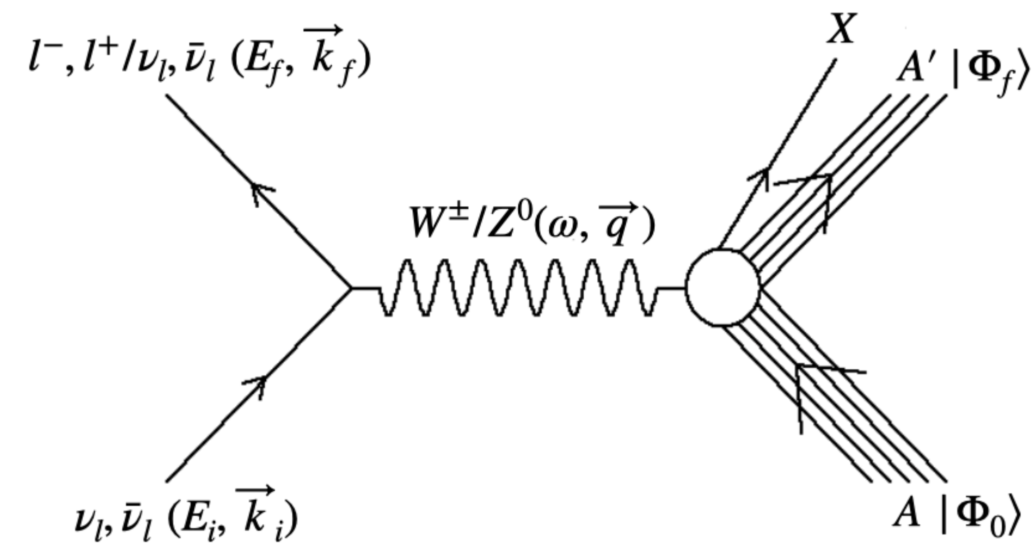

$$\sum_{fi} |\mathscr{M}|^2 \propto \frac{G_F^2}{2} L_{\mu\nu} W^{\mu\nu}$$

Leptonic Tensor: $L_{\mu\nu} = \sum_{fi} (\mathscr{J}_{l,\mu})^\dagger \mathscr{J}_{l,\nu}$ Hadronic Tensor: $W^{\mu\nu} = \sum_{fi} (\mathscr{J}_n^\mu)^\dagger \mathscr{J}_n^\nu$

Transition Amplitude: $\mathscr{J}_n^\mu = \langle \Phi_0 | \hat{J}_n^\mu(q) | \Phi_0 \rangle$

Cross Section:

$$d\sigma \propto \frac{G_F^2}{4\pi} Q_W^2 F_W^2(q)$$

Transition Amplitude: $\mathscr{J}_n^\mu = \langle \Phi_f | \hat{J}_n^\mu(q) | \Phi_0 \rangle$

Cross Section:

$$d\sigma \propto \frac{G_F^2}{4\pi} \sum_{J^\pi} [v_{CC} W_{CC} + v_{CL} W_{CL} + v_{LL} W_{LL} + v_T W_T \pm v_{T'} W_{T'}]$$

Fermilab

- **Cross section (tree level):**

$$\frac{d\sigma}{dT} = \frac{G_F^2}{\pi} M_A \left[1 - \frac{T}{E_i} - \frac{M_A T}{2E_i^2}\right] \frac{Q_W^2}{4} F_W^2(q)$$

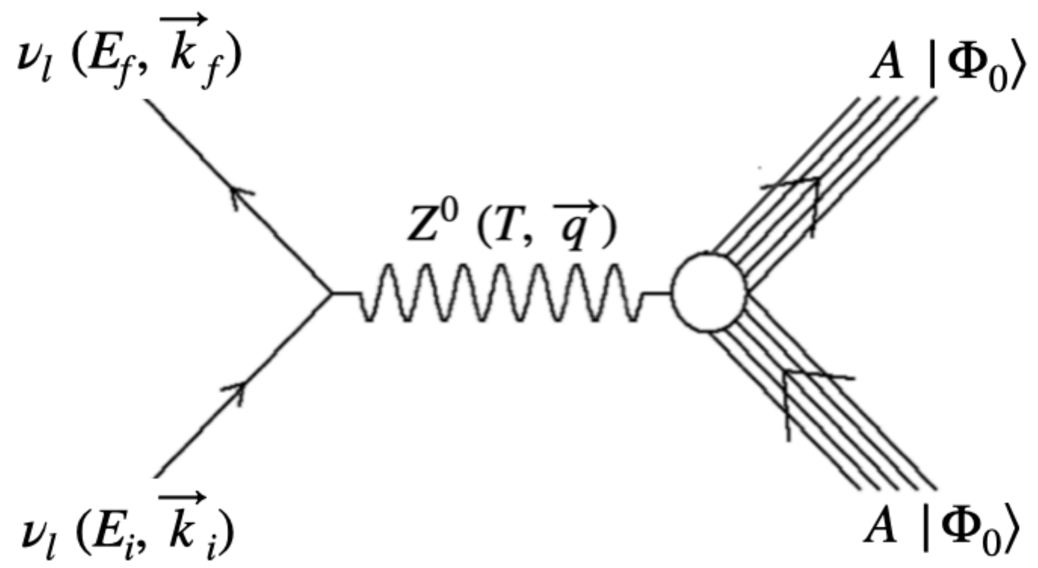

$$T \in \left[0, \frac{2E_i^2}{(M_A + 2E_i)}\right]$$

$$Q_W^2 = [g_n^V N + g_p^V Z]^2$$

CEvNS Cross Section and Form Factors

- **Cross section (tree level):**

$$\frac{d\sigma}{dT} = \frac{G_F^2}{\pi} M_A \left[1 - \frac{T}{E_i} - \frac{M_A T}{2E_i^2}\right] \frac{Q_W^2}{4} F_W^2(q)$$

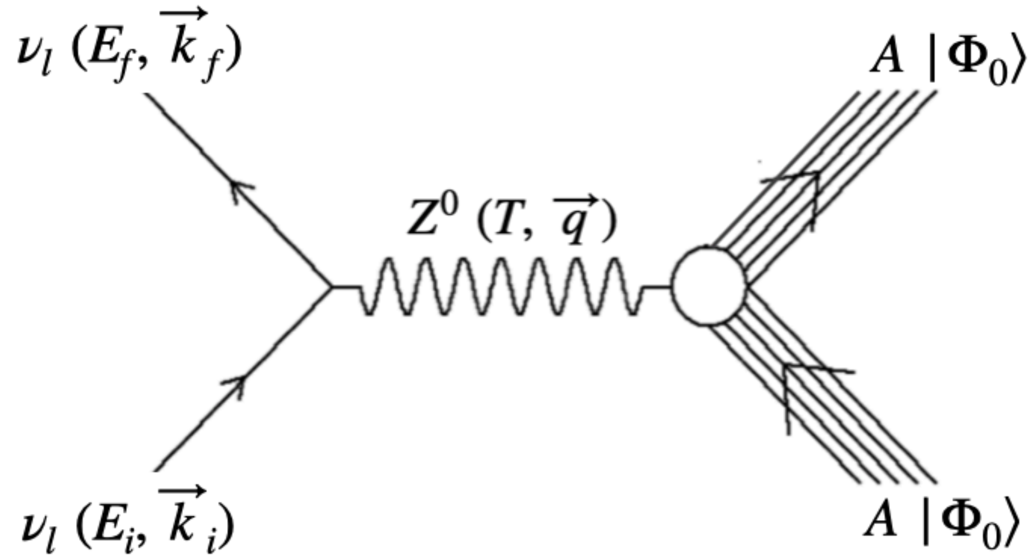

- **Weak Form Factor:**

$$\begin{aligned} Q_W\ F_W(q) &\approx \langle \Phi_0 | \hat{J}_0(q) | \Phi_0 \rangle \\ &\approx \left(1 - 4\sin^2\theta_W\right) Z\ F_p(q) - N\ F_n(q) \\ &\approx 2\pi \int d^3r\ \left[(1 - 4\sin^2\theta_W)\ \rho_p(r) - \rho_n(r)\ \right] j_0(qr) \end{aligned}$$

$$T \in \left[0, \frac{2E_i^2}{(M_A + 2E_i)}\right]$$

$$Q_W^2 = [g_n^V N + g_p^V Z]^2$$

Charge density and charge form factor: proton densities and charge form factors are well know through decades of elastic electron scattering experiments.

Neutron densities and neutron form factor: neutron densities and form factors are poorly known. Note that CEvNS is primarily sensitive to neutron density distributions $(1 - 4\sin^2\theta_W \approx 0)$.

CEvNS and PVES Experimental Measurements

- **Electroweak probes** such as parity–violating electron scattering (**PVES**) and **CEvNS** provide relatively model-independent ways of determining weak form factor and neutron distributions.

T. W. Donnelly, J. Dubach and I. Sick,, Nucl. Phys. A 503, 589-631 (1989).

- **CEvNS Cross Section**

$$\frac{d\sigma}{dT} = \frac{G_F^2}{\pi} M_A \left[1 - \frac{T}{E_i} - \frac{M_A T}{2E_i^2}\right] \frac{Q_W^2}{4} F_W^2(q)$$

- **PVES Asymmetry**

$$A_{pv} = \frac{d\sigma/d\Omega_+ - d\sigma/d\Omega_-}{d\sigma/d\Omega_+ + d\sigma/d\Omega_-} = \frac{G_F q^2 |Q_W|}{4\pi\alpha\sqrt{2}Z} \frac{F_W(q)}{F_{ch}(q^2)}$$

- Both processes are described in first order perturbation theory via the exchange of an electroweak gauge boson between a lepton and a nucleus.
- CEvNS: the lepton is a neutrino and a Z^0 boson is exchanged.
- PVES: the lepton is an electron, but measuring the asymmetry allows one to select the interference between the γ and Z^0 exchange.
- As a result, both the CEvNS cross section and the PVES asymmetry depend on the weak form factor $F_W(Q^2)$, which is mostly determined by the neutron distribution within the nucleus.

CEvNS and PVES Experimental Measurements

- **Electroweak probes** such as parity–violating electron scattering (**PVES**) and **CEvNS** provide relatively model-independent ways of determining weak form factor and neutron distributions.

T. W. Donnelly, J. Dubach and I. Sick,, Nucl. Phys. A 503, 589-631 (1989).

- **CEvNS Cross Section**

D. Z. Freedman, Phys. Rev. D 9, 1389-1392 (1974)

"Freedman declared that the experimental detection of CEvNS would be an "act of hubris" due to the associated "grave experimental difficulties".

- The maximum recoil energy

$$T_{\max} = \frac{E_\nu}{1 + M_A/(2E_\nu)}$$

- **PVES Asymmetry**

CEvNS and PVES Experimental Measurements

- **Electroweak probes** such as parity–violating electron scattering (**PVES**) and **CEvNS** provide relatively model-independent ways of determining weak form factor and neutron distributions.

• CEvNS Cross Section

$$\frac{d\sigma}{dT} = \frac{G_F^2}{\pi} M_A \left[1 - \frac{T}{E_i} - \frac{M_A T}{2E_i^2}\right] \frac{Q_W^2}{4} F_W^2(q)$$

COHERENT Collaboration at SNS at ORNL

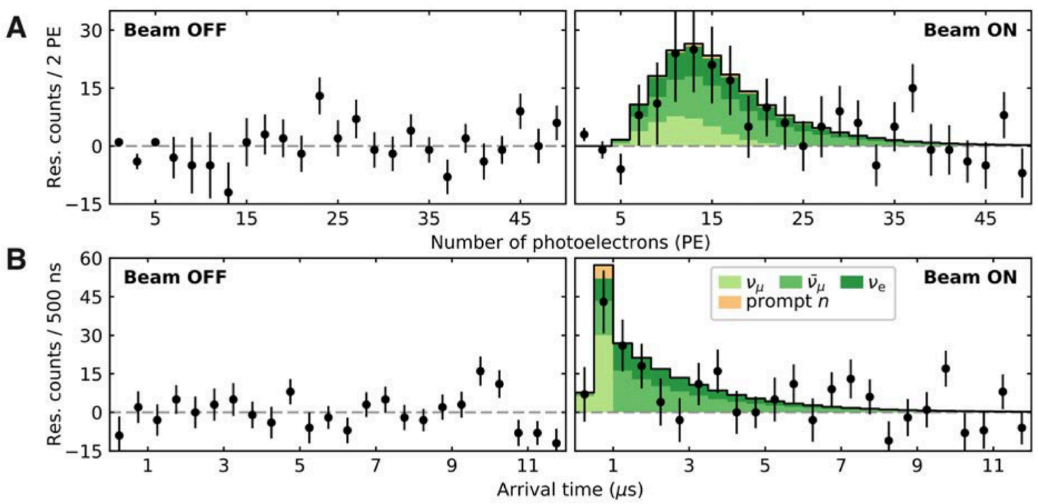

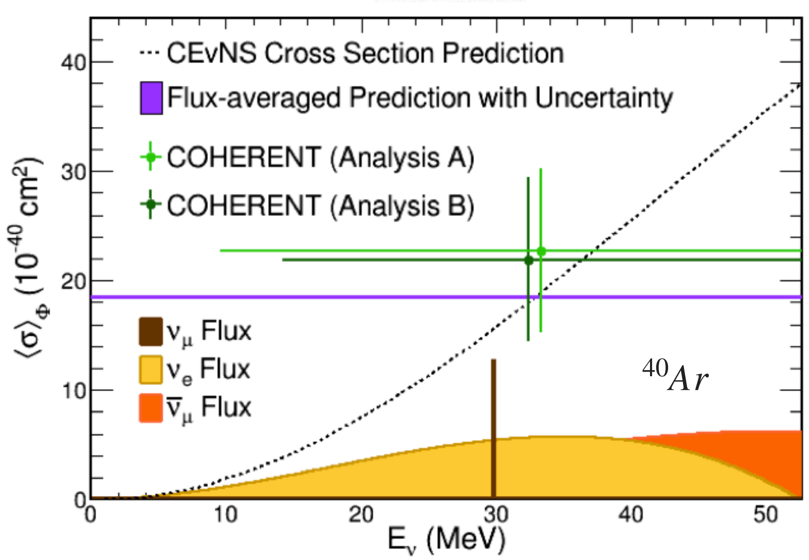

Science 357, 6356, 1123-1126 (2017)
Phys. Rev. Lett. 126, 012002 (2021)

• PVES Asymmetry

Fermilab

CEvNS and PVES Experimental Measurements

- **Electroweak probes** such as parity–violating electron scattering (**PVES**) and **CEvNS** provide relatively model-independent ways of determining weak form factor and neutron distributions.

• CEvNS Cross Section

$$\frac{d\sigma}{dT} = \frac{G_F^2}{\pi} M_A \left[1 - \frac{T}{E_i} - \frac{M_A T}{2E_i^2} \right] \frac{Q_W^2}{4} F_W^2(q)$$

COHERENT Collaboration at SNS at ORNL

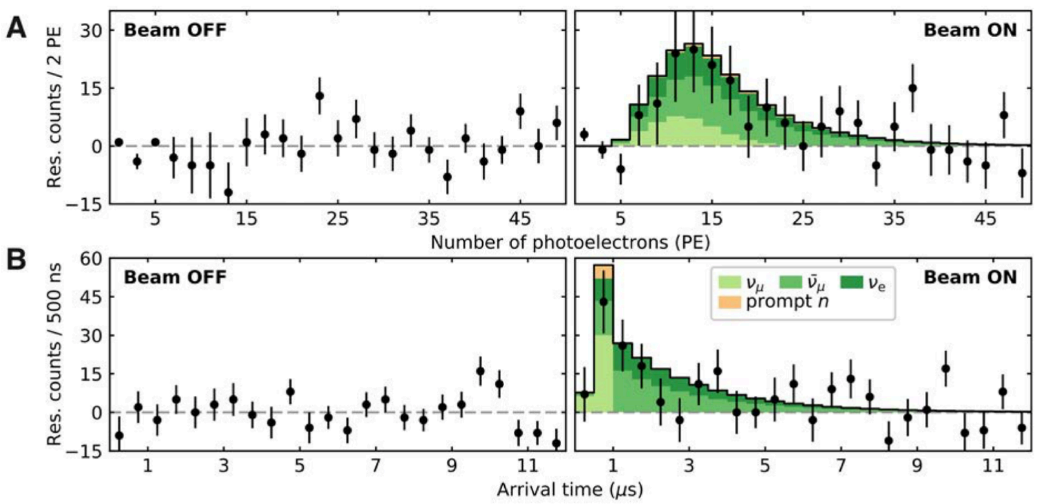

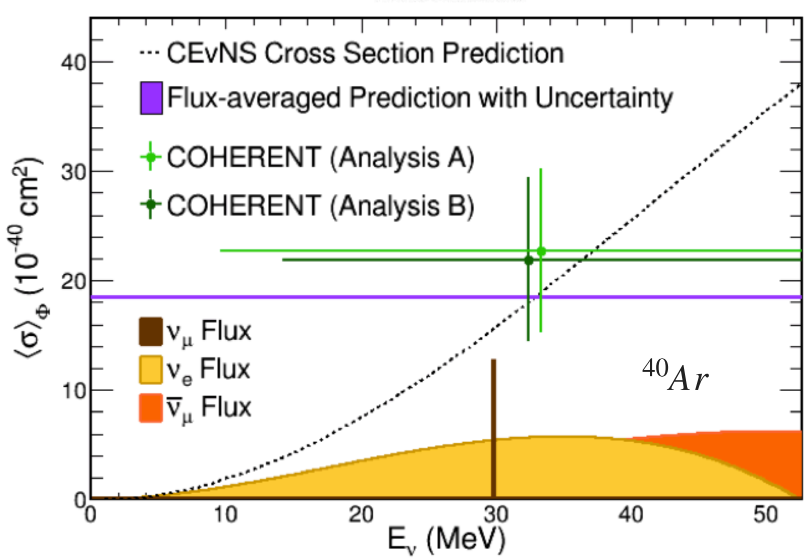

Science 357, 6356, 1123-1126 (2017)
Phys. Rev. Lett. 126, 012002 (2021)

• PVES Asymmetry

- The parity violating asymmetry for elastic electron scattering is the fractional difference in cross section for positive helicity and negative helicity electrons.

$$A_{pv} = \frac{d\sigma/d\Omega_+ - d\sigma/d\Omega_-}{d\sigma/d\Omega_+ + d\sigma/d\Omega_-} = \frac{G_F q^2 |Q_W|}{4\pi\alpha\sqrt{2}Z} \frac{F_W(q)}{F_{ch}(q^2)}$$

- Here F_{ch} is the charge form factor that is typically known from unpolarized electron scattering. Therefore, one can extract F_W from the measurement of A_{PV}.

Experiment	Target	q^2 (GeV^2)	A_{pv} (ppm)
PREX	^{208}Pb	0.00616	0.550 ± 0.018
CREX	^{48}Ca	0.0297	
Qweak	^{27}Al	0.0236	2.16 ± 0.19
MREX	^{208}Pb	0.0073	

arXiv:2203.06853 [hep-ex]

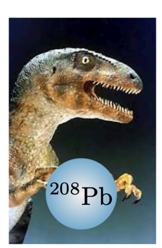

Pb Radius Experiment (PREX)

Calcium Radius Experiment (CREX)

Mainz Radius Experiment (MREX) At P2 experimental hall with ^{208}Pb

Fermilab

CEvNS Cross Section Calculations: HF-SkE2

- Nuclear ground state described as a many-body quantum mechanical system where nucleons are bound in an effective nuclear potential.
- Solve Hartree-Fock (**HF**) equation with a Skyrme (**SkE2**) nuclear potential to obtain single–nucleon wave functions for the bound nucleons in the nuclear ground state.
- Evaluate proton and neutron density distributions and form factors

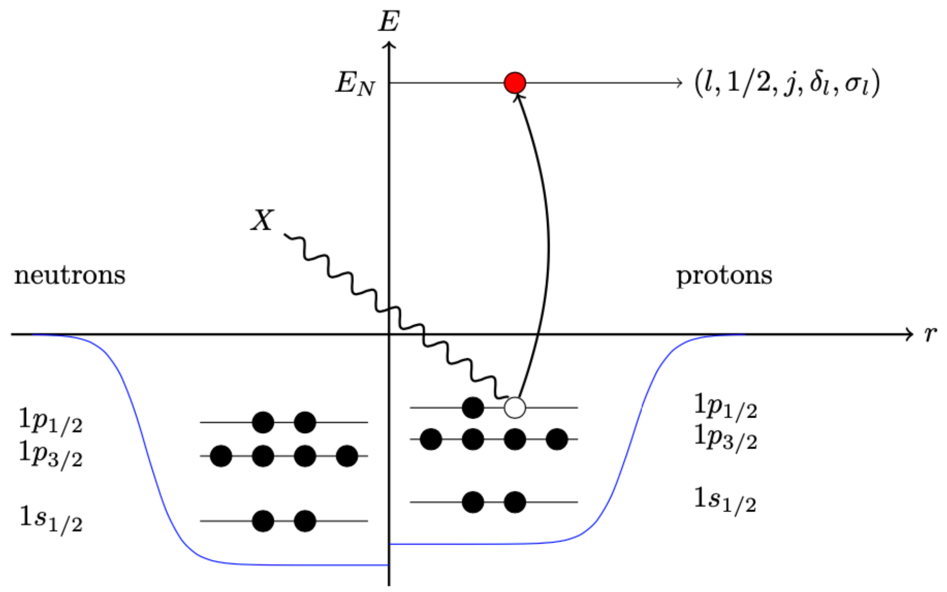

$$\rho_\tau(r) = \frac{1}{4\pi r^2} \sum_\alpha v^2_{\alpha,\tau}\,(2j_\alpha + 1)\,|\,\phi_{\alpha,\tau}(r)\,|^2 \qquad F_\tau(q) = \frac{1}{N}\int d^3r\; j_o(qr)\;\rho_\tau(r)$$

$$(\alpha \in n_\alpha, l_\alpha, j_\alpha)$$

$$(\tau = p, n)$$

CEvNS Cross Section Calculations: HF-SkE2

- Nuclear ground state described as a many-body quantum mechanical system where nucleons are bound in an effective nuclear potential.
- Solve Hartree-Fock (**HF**) equation with a Skyrme (**SkE2**) nuclear potential to obtain single–nucleon wave functions for the bound nucleons in the nuclear ground state.
- Evaluate proton and neutron density distributions and form factors

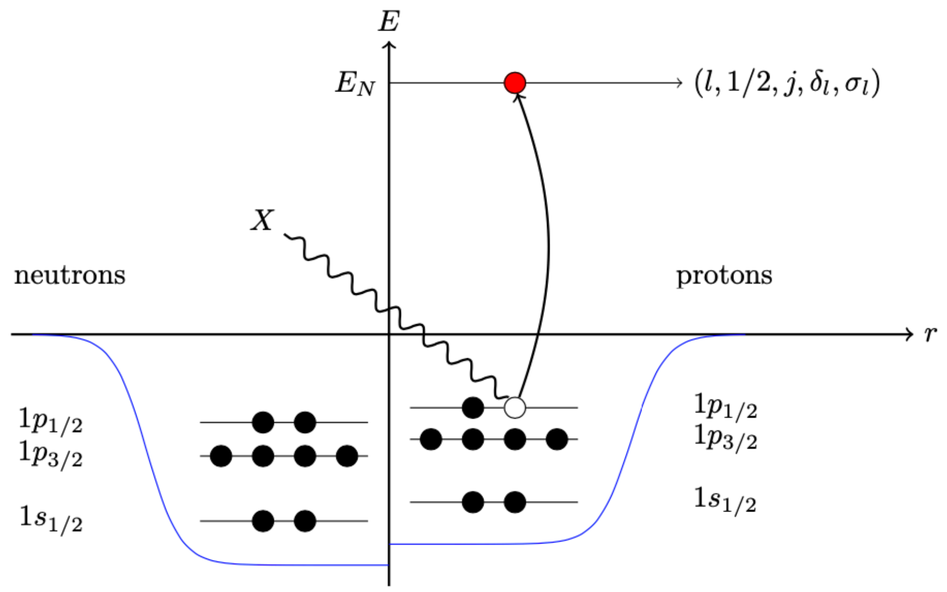

$$\rho_\tau(r) = \frac{1}{4\pi r^2} \sum_\alpha v^2_{\alpha,\tau} \, (2j_\alpha + 1) \, |\, \phi_{\alpha,\tau}(r) \,|^2 \qquad F_\tau(q) = \frac{1}{N} \int d^3r \; j_o(qr) \; \rho_\tau(r)$$

$(\alpha \in n_\alpha, l_\alpha, j_\alpha)$

$(\tau = p, n)$

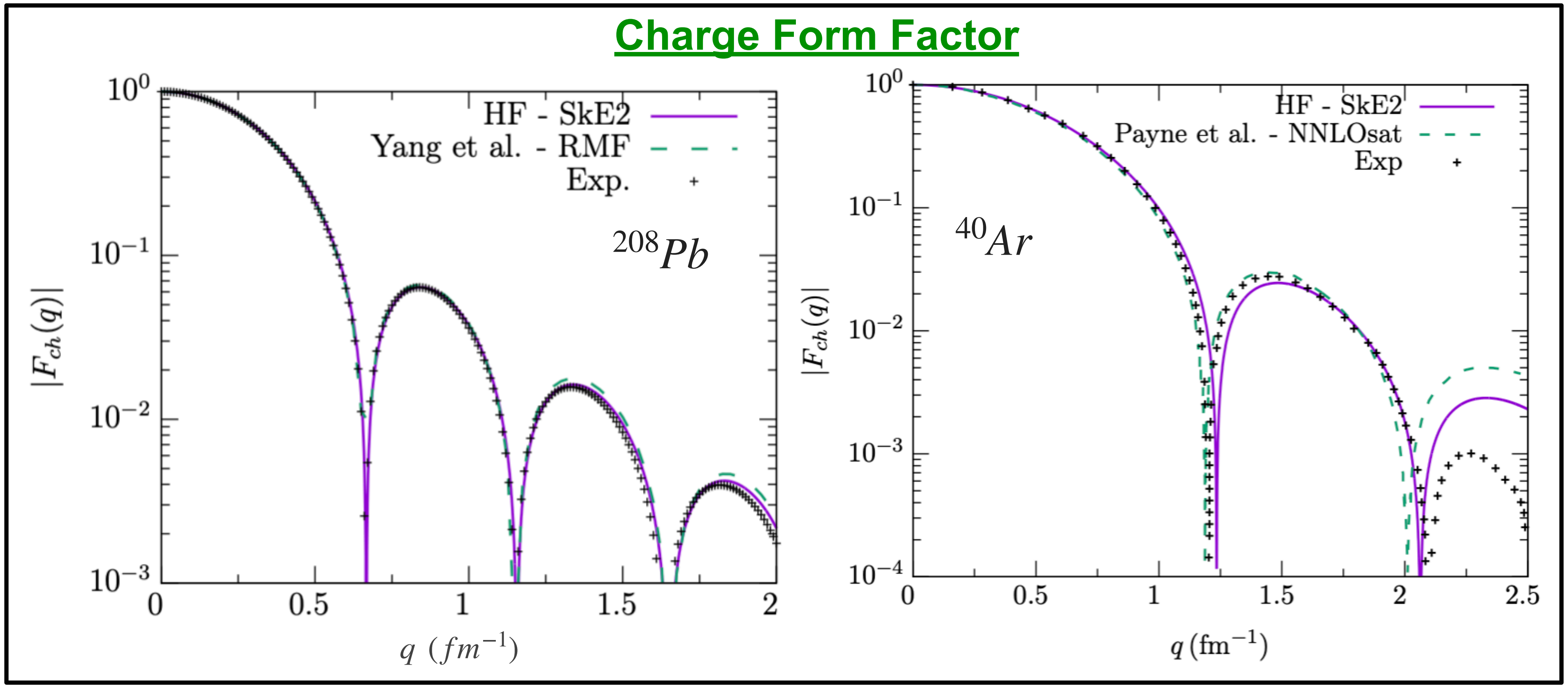

N. Van Dessel, VP, H. Ray and N. Jachowicz, Universe 9, 207 (2023)

Data: H. De Vries, et al., Atom. Data Nucl. Data Tabl. 36, 495 (1987), C. R. Ottermann et al., Nucl. Phys. A 379, 396 (1982)

CEvNS Cross Section Calculations: HF-SkE2

- Nuclear ground state described as a many-body quantum mechanical system where nucleons are bound in an effective nuclear potential.
- Solve Hartree-Fock (**HF**) equation with a Skyrme (**SkE2**) nuclear potential to obtain single–nucleon wave functions for the bound nucleons in the nuclear ground state.
- Evaluate proton and neutron density distributions and form factors

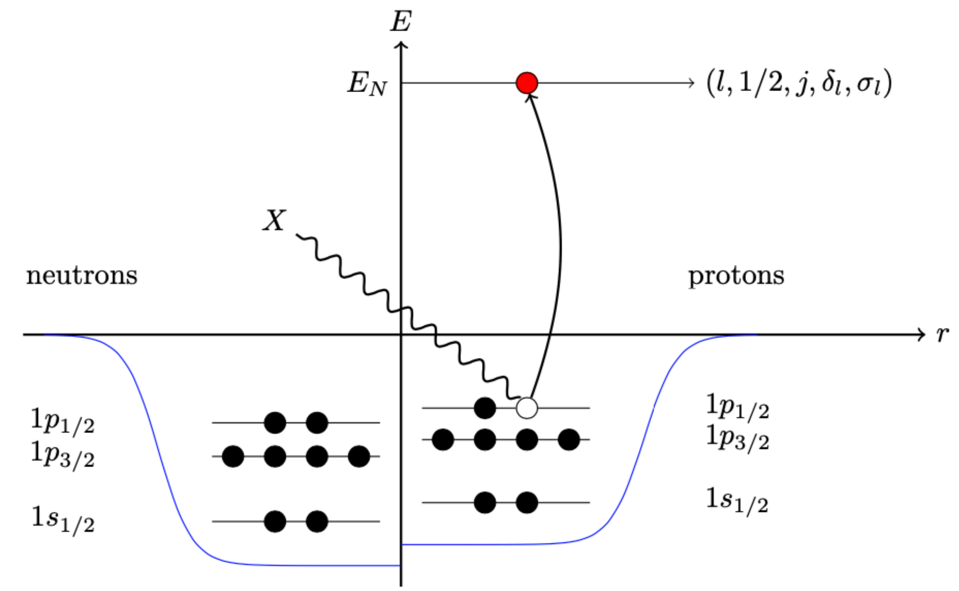

$$\rho_\tau(r) = \frac{1}{4\pi r^2} \sum_\alpha v^2_{\alpha,\tau} \, (2j_\alpha + 1) \, |\, \phi_{\alpha,\tau}(r) \,|^2 \qquad F_\tau(q) = \frac{1}{N} \int d^3r \; j_o(qr) \; \rho_\tau(r)$$

$(\alpha \in n_\alpha, l_\alpha, j_\alpha)$

$(\tau = p, n)$

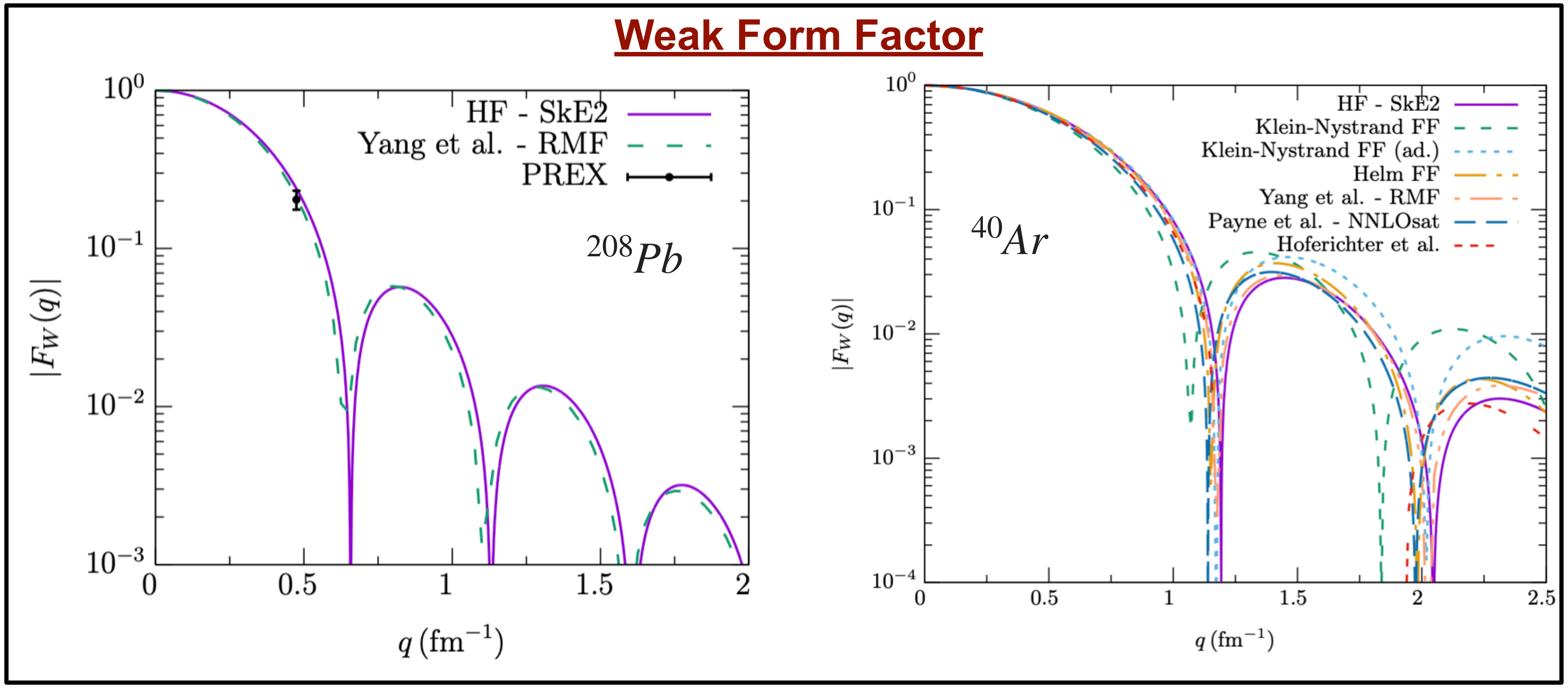

N. Van Dessel, VP, H. Ray and N. Jachowicz, Universe 9, 207 (2023)

Data: S. Abrahamyan et al., Phys. Rev. Lett. 108, 112502 (2012)

CEvNS Cross Section Calculations: HF-SkE2

- Differential cross section on ^{40}Ar, as a function of recoil energy T and scattering angle $\cos\theta_f$.
- The effects of nuclear structure physics are more prominent as the neutrino energy increases.
- Most of the cross section strength lies in the lower-end of the recoil energy and in the forward scattering as the cross section falls off rapidly at higher T (top panels) and higher θ_f values (bottom panels).

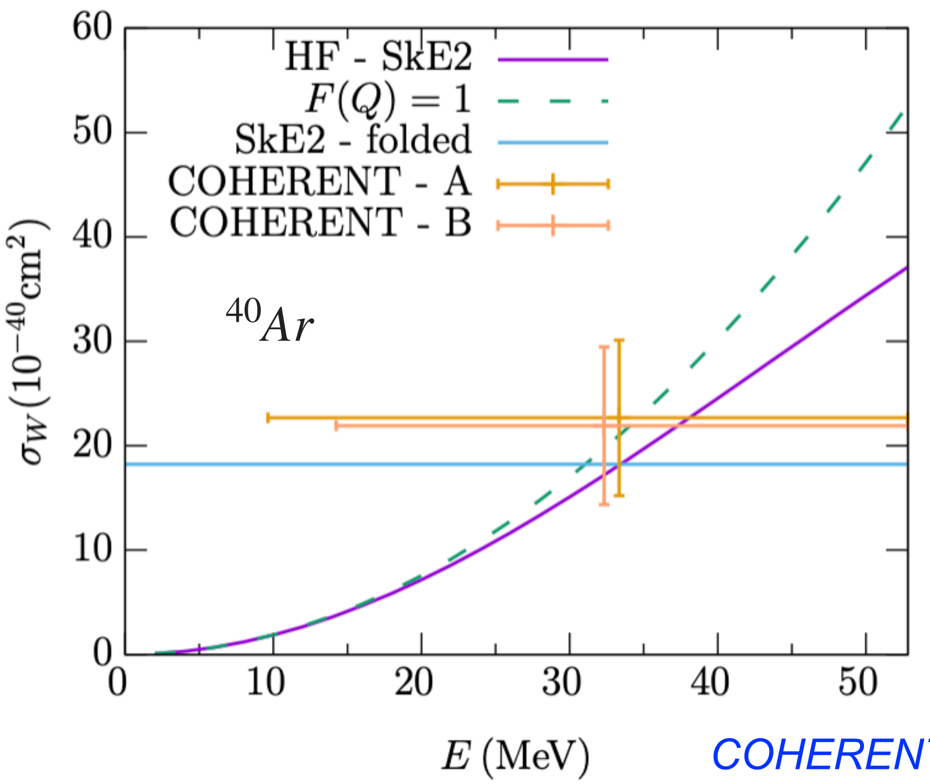

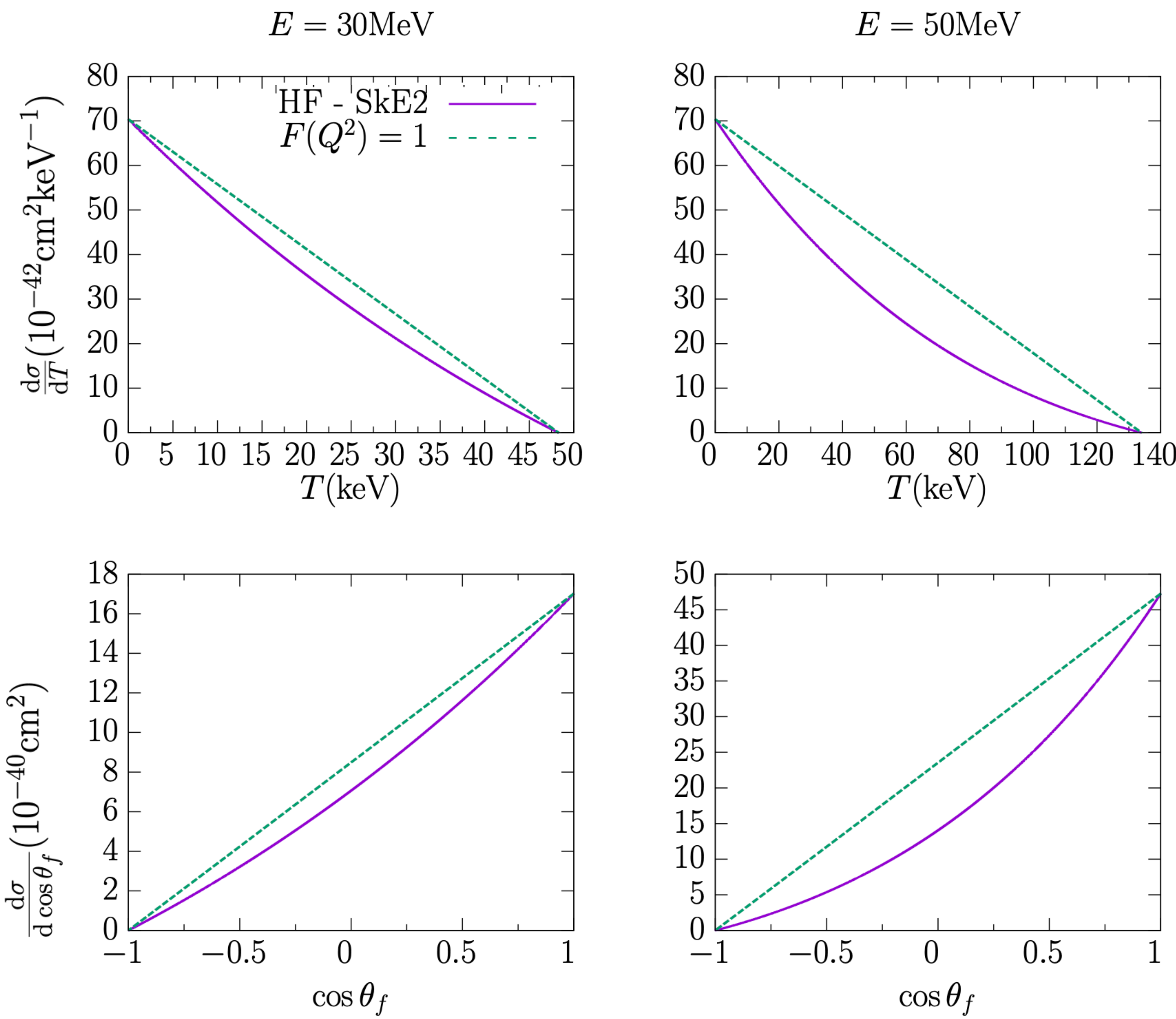

N. Van Dessel, VP, H. Ray and N. Jachowicz, Universe 9, 207 (2023)

COHERENT data: arXiv:2003.10630 [nucl-ex].

CEvNS Cross Section Theory Uncertainty

- With no experimental data to constrain neutron distributions and weak nuclear form factors. We will try to asses a theoretical uncertainty on ^{40}Ar weak form factor and ^{40}Ar CEvNS cross section by comparing **Six** theory predictions.

A. Four microscopic many-body nuclear theory approaches that describe an accurate picture of the nuclear ground state and nucleon densities.

- The HF–SkE2 model
- Model of Payne *et al.* [Phys. Rev. C 100, 061304 (2019)] where form factors are calculated within a coupled-cluster theory from first principles using a chiral NNLO$_{sat}$ interaction.
- Model of Yang *et al.* [Phys. Rev. C 100, 054301 (2019)] where form factors are predicted within a relativistic mean–field model informed by the properties of finite nuclei and neutron stars.
- Model of Hoferichter *et al.* [arXiv:2007.08529 [hep-ph]] where form factors are calculated within a large-scale nuclear shell model.

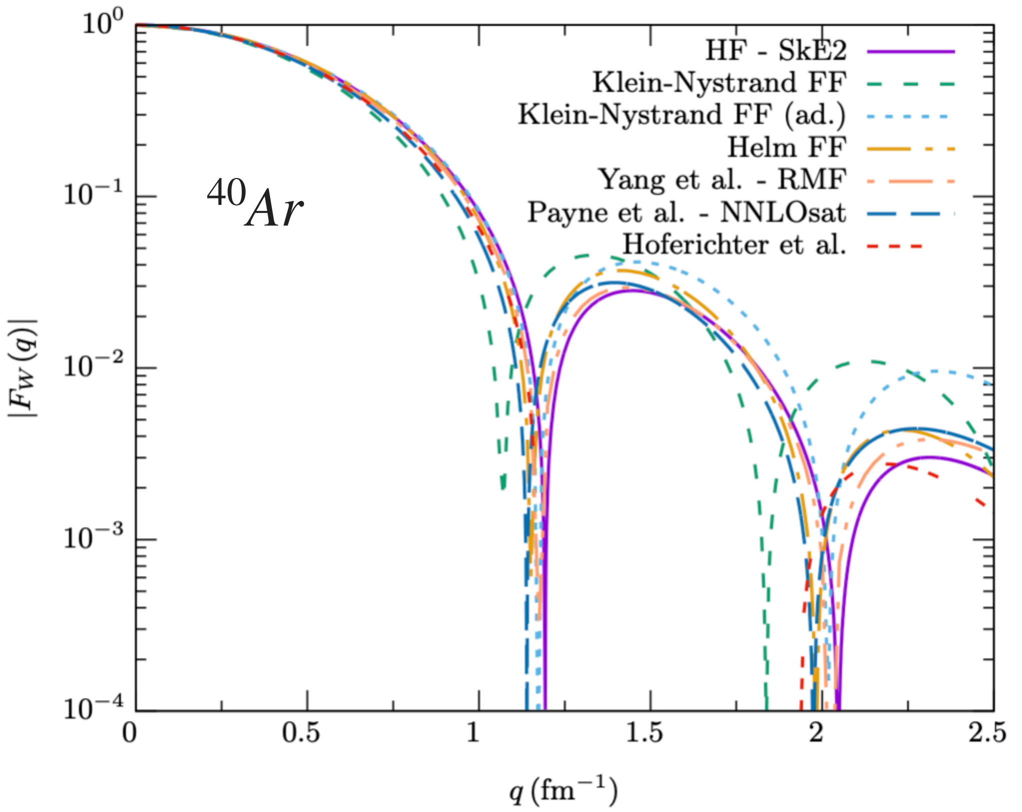

N. Van Dessel, VP, H. Ray and N. Jachowicz, Universe 9, 207 (2023)

B. Two phenomenological approaches where density distributions are represented by analytical expressions, widely used in the CEvNS community.

One can assume: $\rho_n(r) \approx \rho_p(r)$ and hence $F_n(q) \approx F_p(q) \approx F_A(q)$

- The Helm approach: $$F_{\rm Helm}(q^2) = \frac{3j_1(qR_0)}{qR_0} e^{-q^2 s^2/2}$$
- The Klein–Nystrand (KN) approach: $$F_{\rm KN}(q^2) = \frac{3j_1(qR_A)}{qR_A}\left[\frac{1}{1+q^2 a_k^2}\right]$$

- To quantify differences between different ^{40}Ar form factors and ^{40}Ar CEvNS cross section due to different underlying nuclear structure details. We consider quantities that emphasize the relative differences between the results of different calculations, arbitrarily using HF–SkE2 as a reference calculation, as follows:

$$|\Delta F^i_{\mathrm{W}}(q)| = \frac{|F^i_{\mathrm{W}}(q) - F^{\mathrm{HF}}_{\mathrm{W}}(q)|}{|F^{\mathrm{HF}}_{\mathrm{W}}(q)|}$$

$$\Delta\sigma^i_{\mathrm{W}}(E) = \frac{|\sigma^i_{\mathrm{W}}(E) - \sigma^{\mathrm{HF}}_{\mathrm{W}}(E)|}{\sigma^{\mathrm{HF}}_{\mathrm{W}}(E)}$$

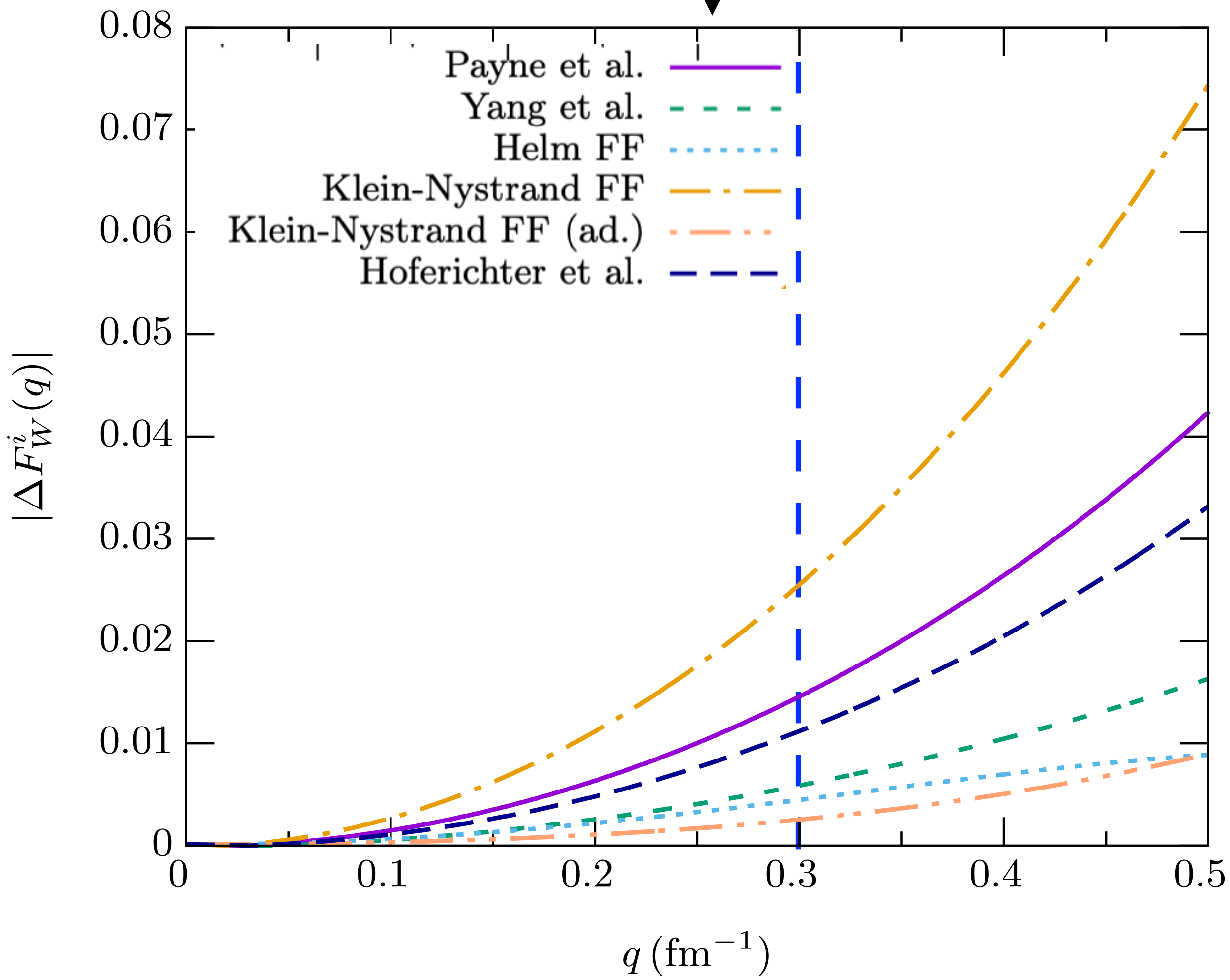

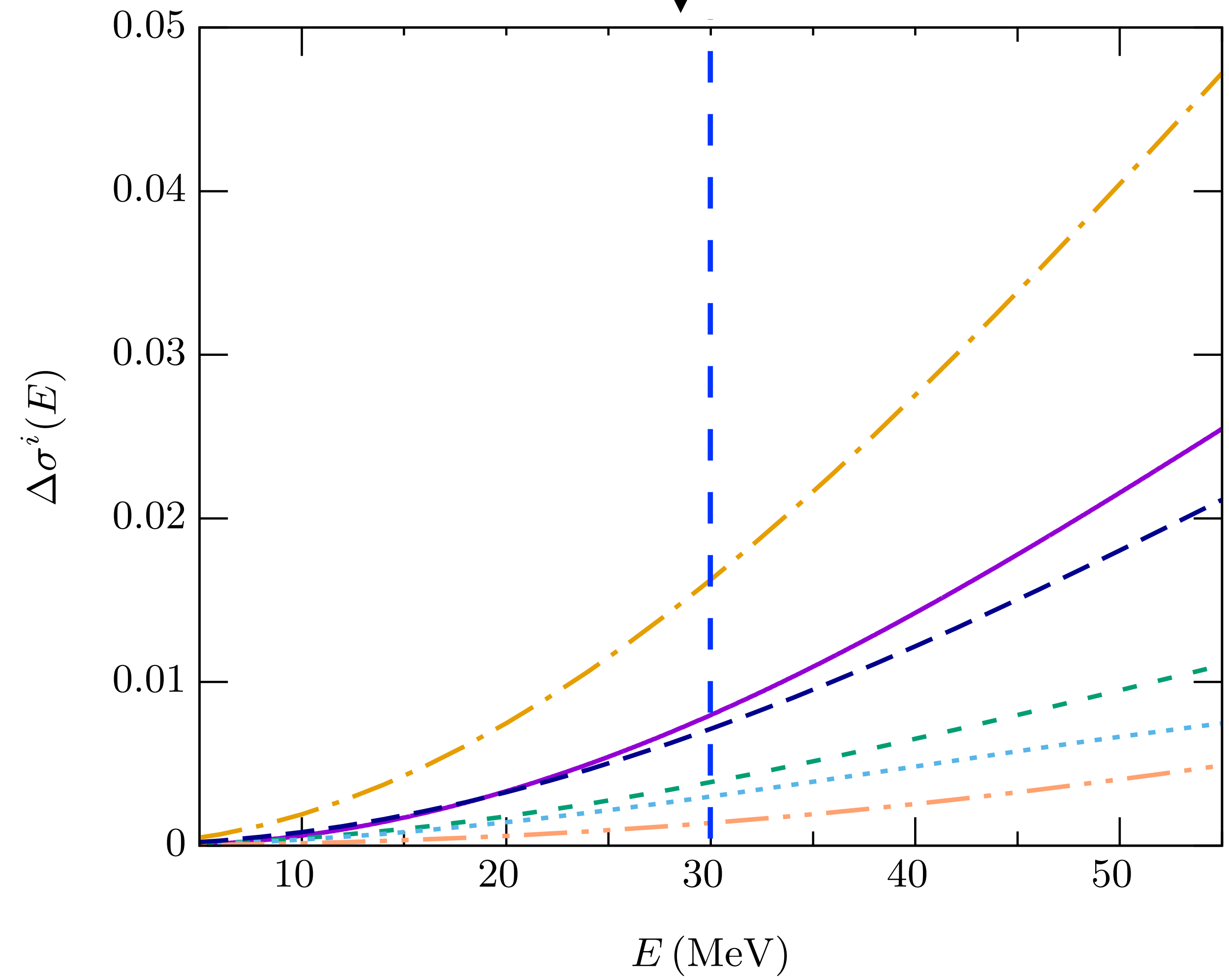

N. Van Dessel, VP, H. Ray and N. Jachowicz, Universe 9, 207 (2023)

CEvNS Cross Section Theory Uncertainty

- In writing down the CEvNS cross section a few subtleties were ignored
  - **Axial-vector operator**: an additional contribution that is not coherently enhanced,

$$\frac{\mathrm{d}\sigma}{\mathrm{d}T} = \frac{G_F^2 M}{4\pi}\left(1 - \frac{MT}{2E_\nu^2} - \frac{T}{E_\nu}\right) Q_\mathrm{W}^2 \left[F_\mathrm{W}(q^2)\right]^2 + \frac{G_F^2 M}{4\pi}\left(1 + \frac{MT}{2E_\nu^2} - \frac{T}{E_\nu}\right) F_A(q^2)$$

The axial-vector form factor, $F_A(q^2)$ depends on the axial charges and radii of the nucleon. This contribution vanishes for spin-zero nuclei such ^{40}Ar.

M. Hoferichter, J. Menendez and A. Schwenk, Phys. Rev. D 102, 074018 (2020)

  - **Radiative Corrections:** At NLO in the electromagnetic coupling constant α, cross section inherits a flavor-dependent contribution entering with a charge form factor of the nucleus.

$$\frac{\mathrm{d}\sigma_{\nu_\ell}}{\mathrm{d}T} = \frac{\mathrm{G_F^2} M_\mathrm{A}}{4\pi}\left(1 - \frac{T}{E_\nu} - \frac{M_\mathrm{A} T}{2E_\nu^2}\right)\left(\mathrm{F_W}\left(Q^2\right) + \frac{\alpha}{\pi}[\delta^{\nu_\ell} + \delta^\mathrm{QCD}]\mathrm{F_{ch}}(Q^2)\right)^2$$

The corrections induced by hadronic and/or quark loops, proportional to δ^{QCD}, are flavor independent, whereas the corrections from charged leptons, proportional to δ^{ν_l}, depend on the neutrino flavor.

O. Tomalak, P. Machado, VP and R. Plestid, JHEP 02, 097 (2021)

CEvNS Cross Section Theory Uncertainty

- Complete theoretical error budget (in %) of CEvNS on 40Ar: includes uncertainties at nuclear, nucleon, hadronic and quark levels separately as well as perturbative error.

E_ν, MeV	Nuclear	Nucleon	Hadronic	Quark	Pert.	Total
50	4.	0.06	0.56	0.13	0.08	4.05
30	1.5.	0.014	0.56	0.13	0.03	1.65
10	0.04	0.001	0.56	0.13	0.004	0.58

- Relative cross section error

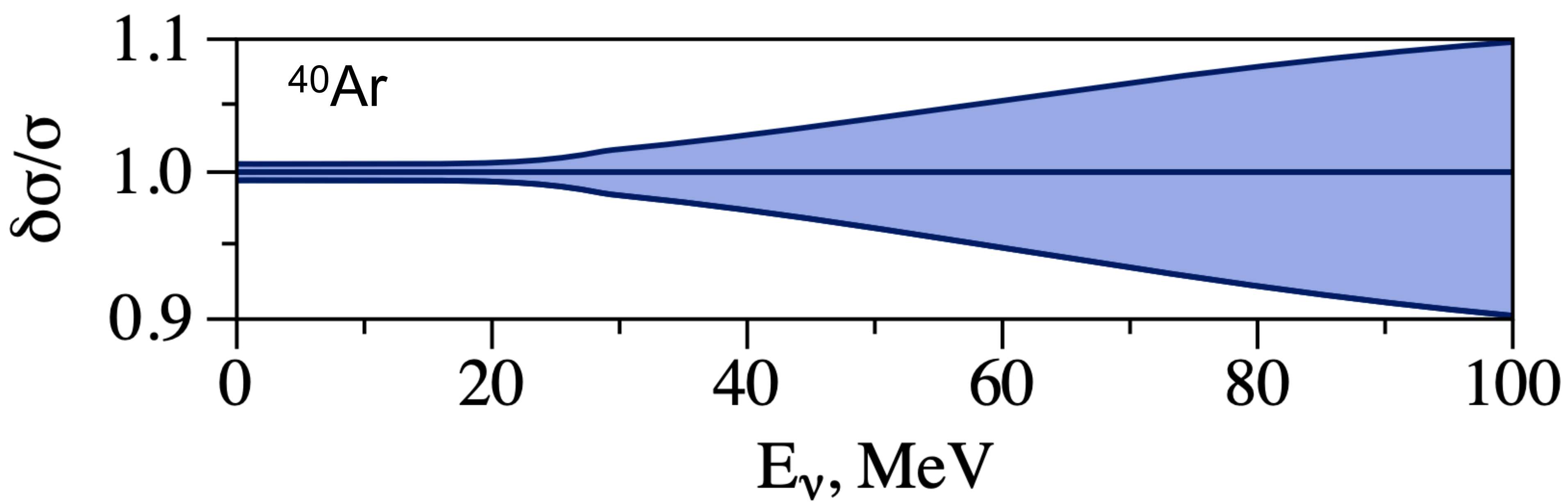

O. Tomalak, P. Machado, VP and R. Plestid, JHEP 02, 097 (2021)

10s of MeV Inelastic Neutrino-Nucleus Scattering

- **Cross Section and Responses**

$$\sum_{fi} |\mathscr{M}|^2 \propto \frac{G_F^2}{2} L_{\mu\nu} W^{\mu\nu}$$

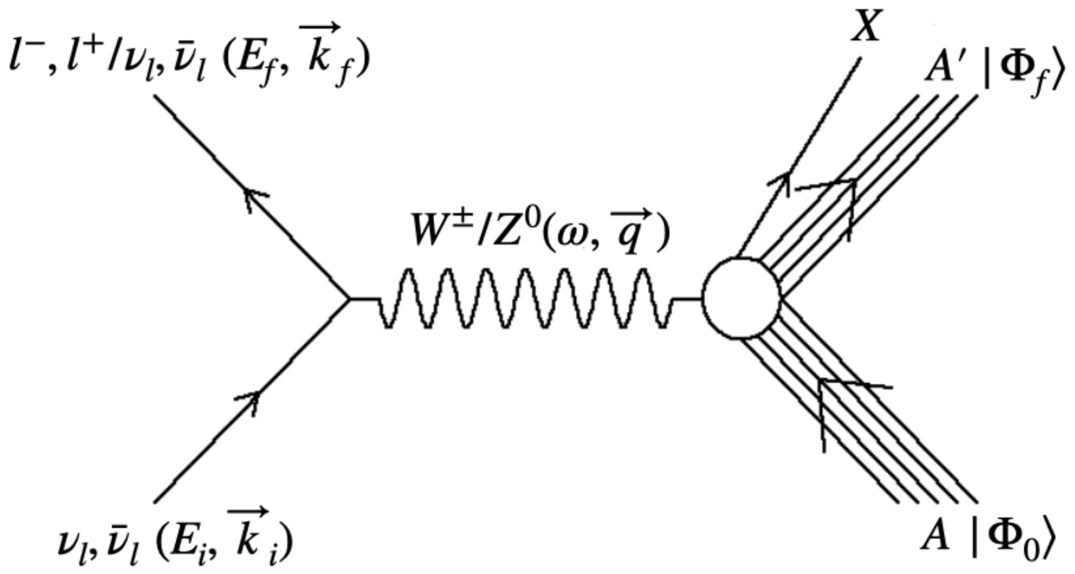

$$\omega = E_i - E_f, \quad q = |\vec{k}_i - \vec{k}_f|, \quad Q^2 = q^2 - \omega^2$$

Cross Section and Responses

$$\sum_{fi} |\mathscr{M}|^2 \propto \frac{G_F^2}{2} L_{\mu\nu} W^{\mu\nu}$$

- Leptonic Tensor: $L_{\mu\nu} = \sum_{fi} (\mathscr{J}_{l,\mu})^\dagger \mathscr{J}_{l,\nu}$
- Hadronic Tensor: $W^{\mu\nu} = \sum_{fi} (\mathscr{J}_n^\mu)^\dagger \mathscr{J}_n^\nu$
- Transition Amplitude: $\mathscr{J}_n^\mu = \langle \Phi_f | \hat{J}_n^\mu(q) | \Phi_0 \rangle$

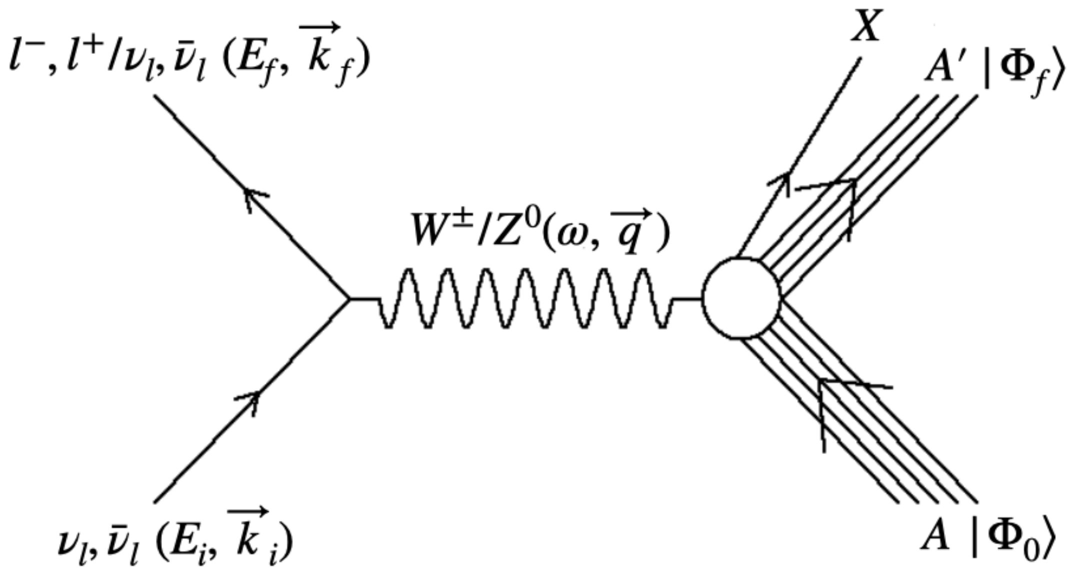

$$\omega = E_i - E_f, \quad q = |\vec{k}_i - \vec{k}_f|, \quad Q^2 = q^2 - \omega^2$$

$$\left(\frac{d^2\sigma}{d\omega_\nu d\Omega}\right)_\nu = \frac{G_F^2 \cos^2\theta_c}{(4\pi)^2} \left(\frac{2}{2J_i+1}\right) \varepsilon_f \kappa_f \times \zeta^2(Z', \varepsilon_f, q_\nu) \left[\sum_{J=0}^{\infty} \sigma_{CL,\nu}^J + \sum_{J=1}^{\infty} \sigma_{T,\nu}^J\right]$$

$$\sigma_{CL,\nu}^J = \left[v_\nu^{\mathcal{M}} R_\nu^{\mathcal{M}} + v_\nu^{\mathcal{L}} R_\nu^{\mathcal{L}} + 2\, v_\nu^{\mathcal{ML}} R_\nu^{\mathcal{ML}}\right]$$

$$\sigma_{T,\nu}^J = \left[v_\nu^T R_\nu^T \pm 2\, v_\nu^{TT} R_\nu^{TT}\right]$$

10s of MeV Inelastic Neutrino-Nucleus Scattering: HF-CRPA Model

- In the inelastic cross section calculations, the influence of long-range correlations between the nucleons is introduced through the continuum Random Phase Approximation (CRPA) on top of the HF-SkE2 approach.

- CRPA effects are vital to describe the process where the nucleus can be excited to low-lying collective nuclear states.

- The local RPA-polarization propagator is obtained by an iteration to all orders of the first order contribution to the particle-hole Green's function.

For details on HF-CRPA model, see V. Pandey's PhD Thesis

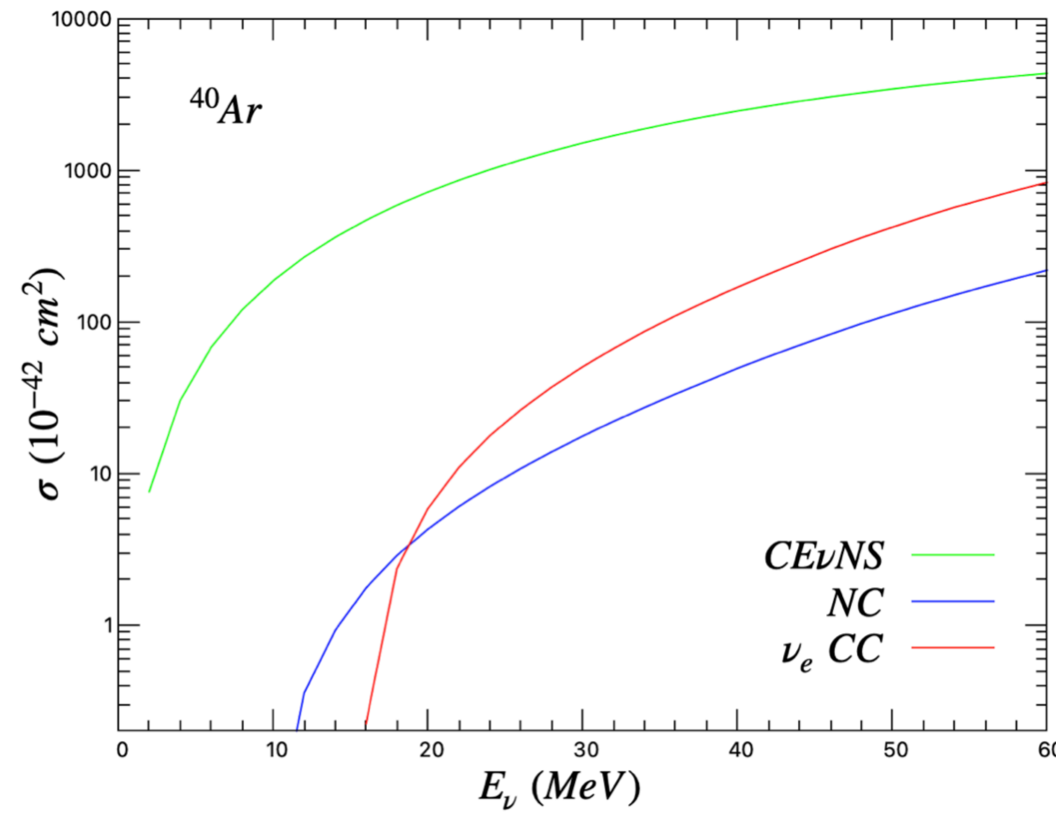

$$\Pi^{(RPA)}(x_1, x_2; E_x) = \Pi^{(0)}(x_1, x_2; E_x) + \frac{1}{\hbar}\int dx dx'\ \Pi^0(x_1, x; E_x) \times \tilde{V}(x, x')\ \Pi^{(RPA)}(x', x_2; E_x)$$

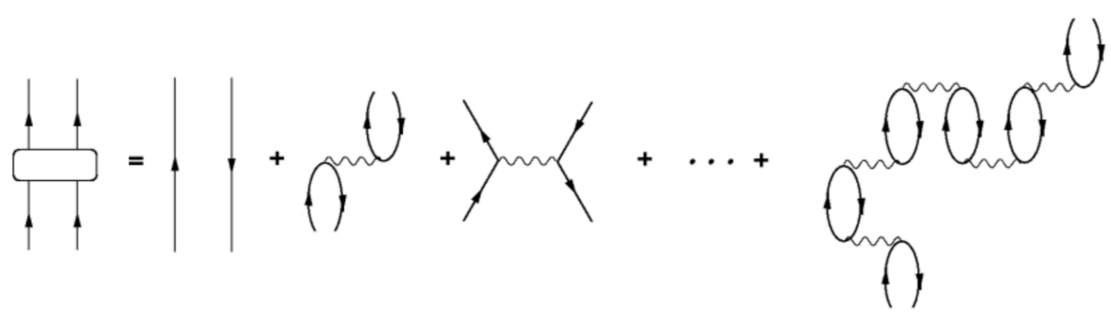

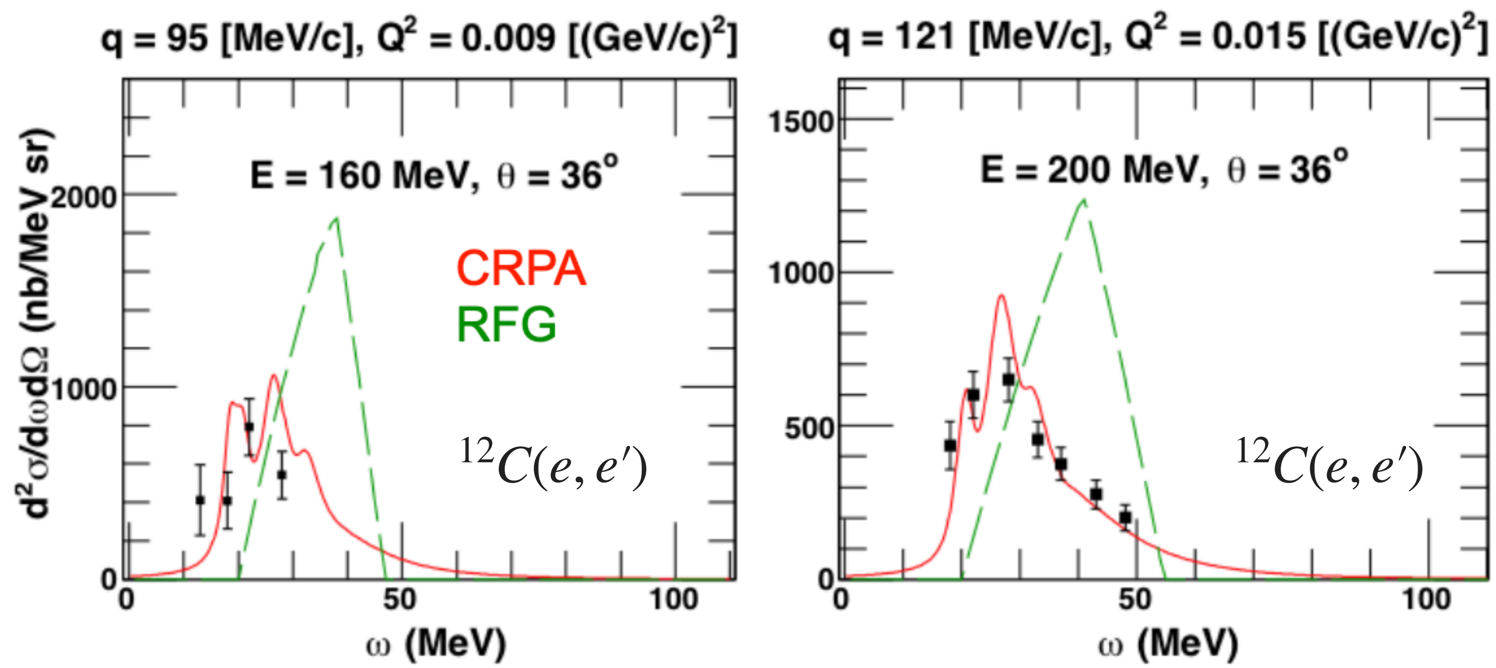

10s of MeV Inelastic Neutrino-Nucleus Scattering: HF-CRPA Model

- In the inelastic cross section calculations, the influence of long-range correlations between the nucleons is introduced through the continuum Random Phase Approximation (CRPA) on top of the HF-SkE2 approach.
- CRPA effects are vital to describe the process where the nucleus can be excited to low-lying collective nuclear states.
- The local RPA-polarization propagator is obtained by an iteration to all orders of the first order contribution to the particle-hole Green's function.

For details on HF-CRPA model, see [V. Pandey's PhD Thesis]

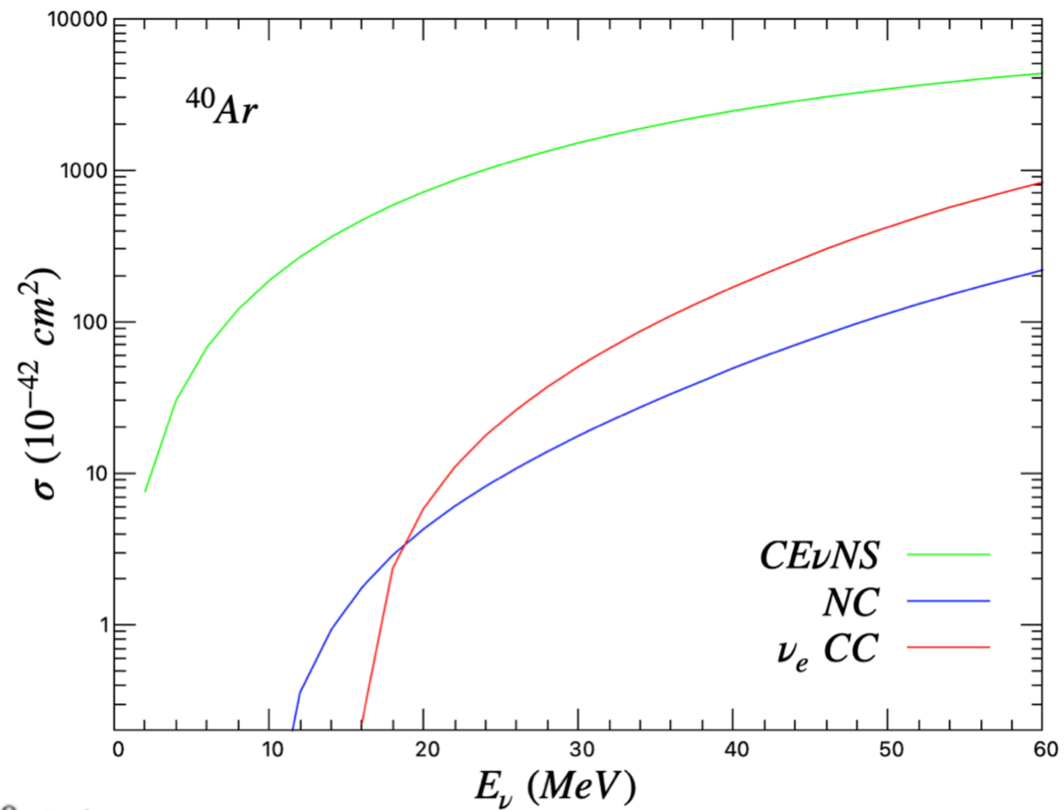

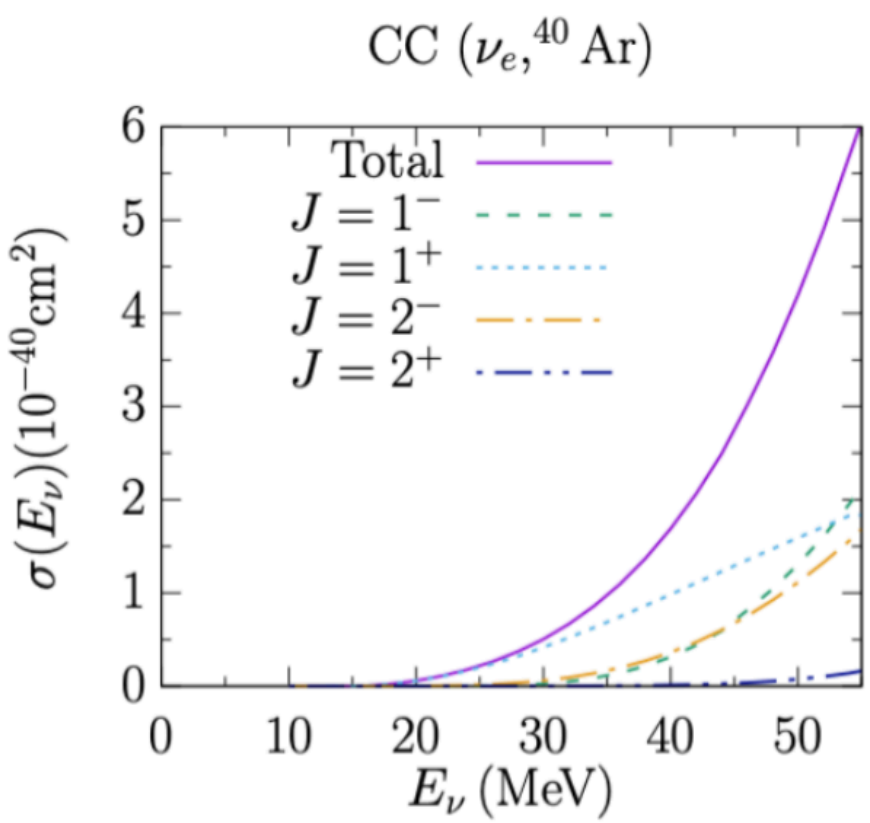

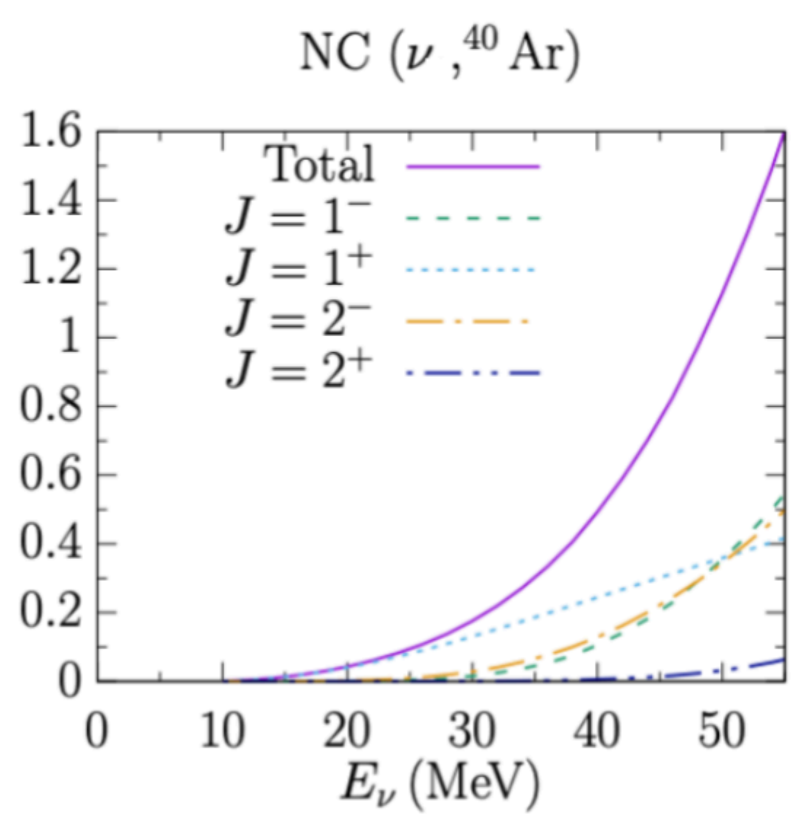

Fermilab

10s of MeV Inelastic Neutrino-Nucleus Scattering: Uncertainty

- **Core-collapse supernova** can be detected in DUNE using e.g. ν_e charge current inelastic neutrino-nucleus scattering process.
- These 10s of MeV neutrinos inelastically scatter off the nucleus, exciting nucleus to its low-lying excitation states, subject to nuclear structure physics.
- The inelastic neutrino-nucleus cross sections are quite poorly understood. There are very few existing measurements, none at better than the 10% uncertainty level. As a result, the uncertainties on the theoretical calculations of, e.g., neutrino-argon cross sections are not well quantified at all at these energies.

Reaction Channel	Experiment	Measurement (10^{-42} cm^2)
$^{12}C(\nu_e, e^-)^{12}N_{g.s.}$	KARMEN	$9.1 \pm 0.5(stat) \pm 0.8(sys)$
	E225	$10.5 \pm 1.0(stat) \pm 1.0(sys)$
	LSND	$8.9 \pm 0.3(stat) \pm 0.9(sys)$
$^{12}C(\nu_e, e^-)^{12}N^*$	KARMEN	$5.1 \pm 0.6(stat) \pm 0.5(sys)$
	E225	$3.6 \pm 2.0(tot)$
	LSND	$4.3 \pm 0.4(stat) \pm 0.6(sys)$
$^{12}C(\nu_\mu, \nu_\mu)^{12}C^*$	KARMEN	$3.2 \pm 0.5(stat) \pm 0.4(sys)$
$^{12}C(\nu, \nu)^{12}C^*$	KARMEN	$10.5 \pm 1.0(stat) \pm 0.9(sys)$
$^{56}Fe(\nu_e, e^-)\ ^{56}Co$	KARMEN	$256 \pm 108(stat) \pm 43(sys)$
$^{127}I(\nu_e, e^-)^{127}Xe$	LSND	$284 \pm 91(stat) \pm 25(sys)$
$^{127}I(\nu_e, e^-)X$	COHERENT	$920^{+2.1}_{-1.8}$
$^{nat}Pb(\nu_e, Xn)$	COHERENT	– –

TABLE III. Flux-averaged cross-sections measured at stopped pion facilties on various nuclei. Experimental data gathered from the LAMPF [89], KARMEN [90–93], E225 [94], LSND [95–97], and COHERENT [98, 99] experiments. Table adapted from the Ref. [9].

V. Pandey, Prog. Part. Nucl. Phys., 104078 (2023)

Past measurements on Carbon

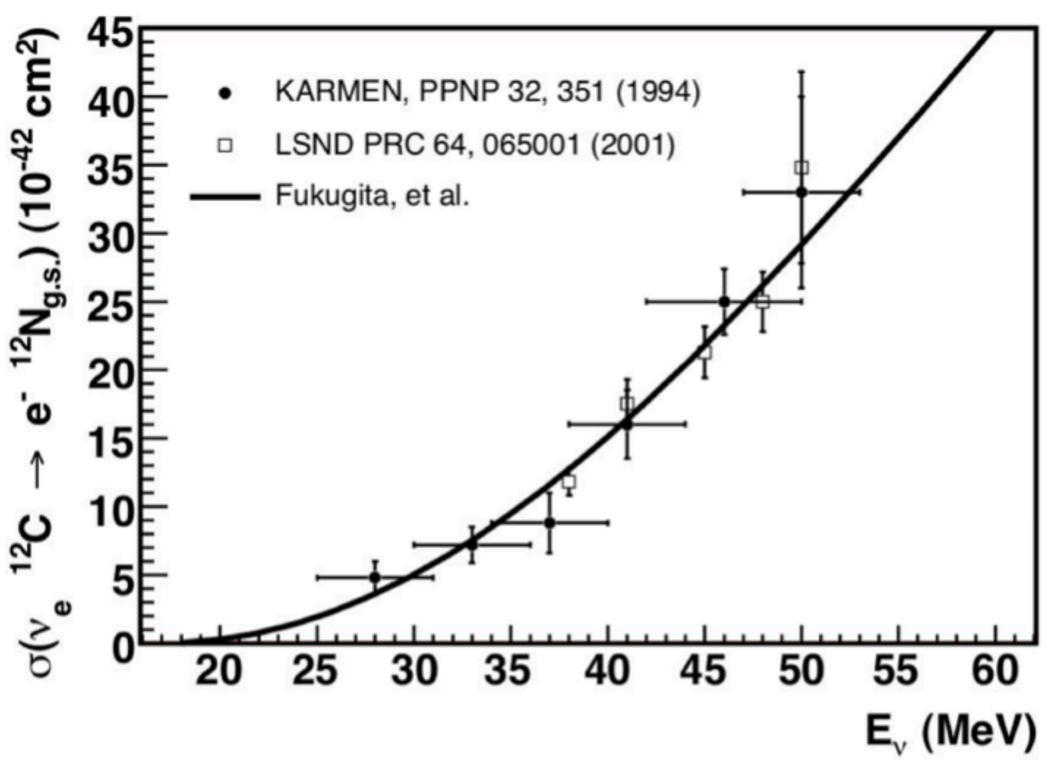

Rev. Mod. Phys. 84,1307 (2012)

10s of MeV Inelastic Neutrino-Nucleus Scattering: Uncertainty

- **Core-collapse supernova** can be detected in DUNE using e.g. ν_e charge current inelastic neutrino-nucleus scattering process.

- These 10s of MeV neutrinos inelastically scatter off the nucleus, exciting nucleus to its low-lying excitation states, subject to nuclear structure physics.

- The inelastic neutrino-nucleus cross sections are quite poorly understood. There are very few existing measurements, none at better than the 10% uncertainty level. As a result, the uncertainties on the theoretical calculations of, e.g., neutrino-argon cross sections are not well quantified at all at these energies.

No measurements on Argon yet

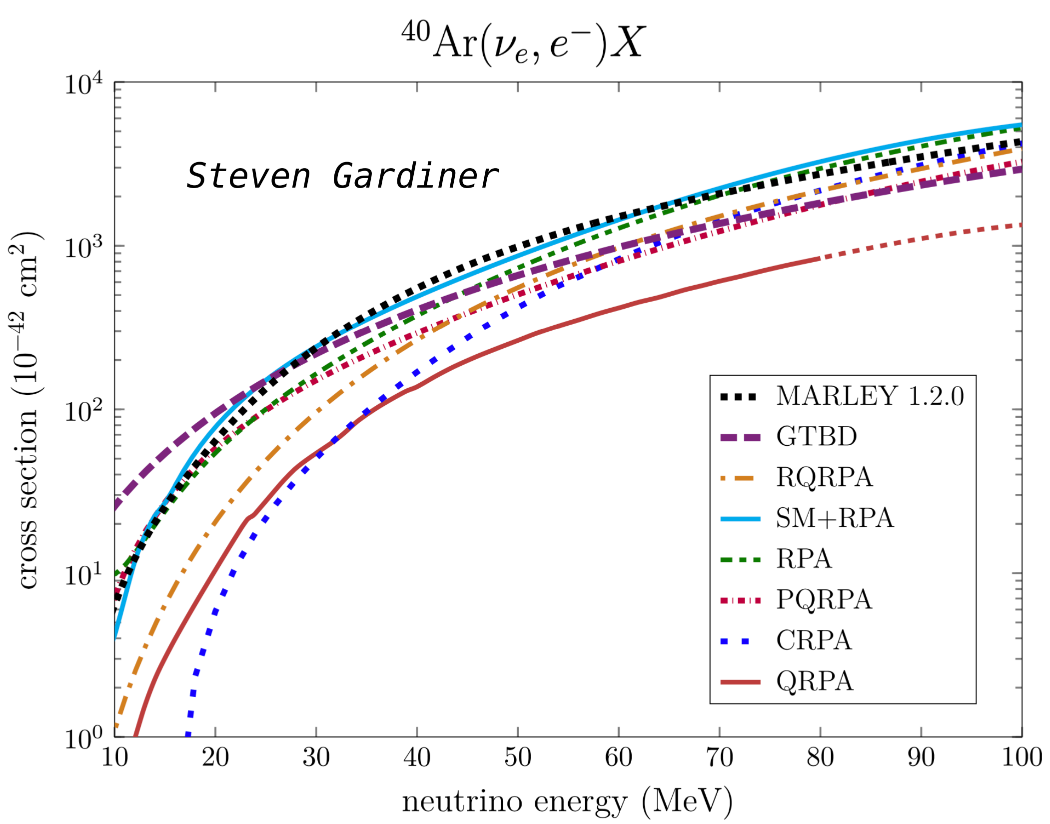

DUNE Collaboration, arXiv:2303.17007 [hep-ex]

“Current understanding of $\sigma(E_\nu)$ is inadequate. Measuring ε energy release (other parameters) to 10% requires 5% (20%) knowledge of the cross section!

10s of MeV Inelastic Neutrino-Nucleus Scattering: Uncertainty

- MARLEY (Model of Argon Reaction Low Energy Yields) is a dedicated low-energy neutrino event generator developed by Steven Gardiner to simulate tens-of-MeV neutrino-nucleus interactions on argon.

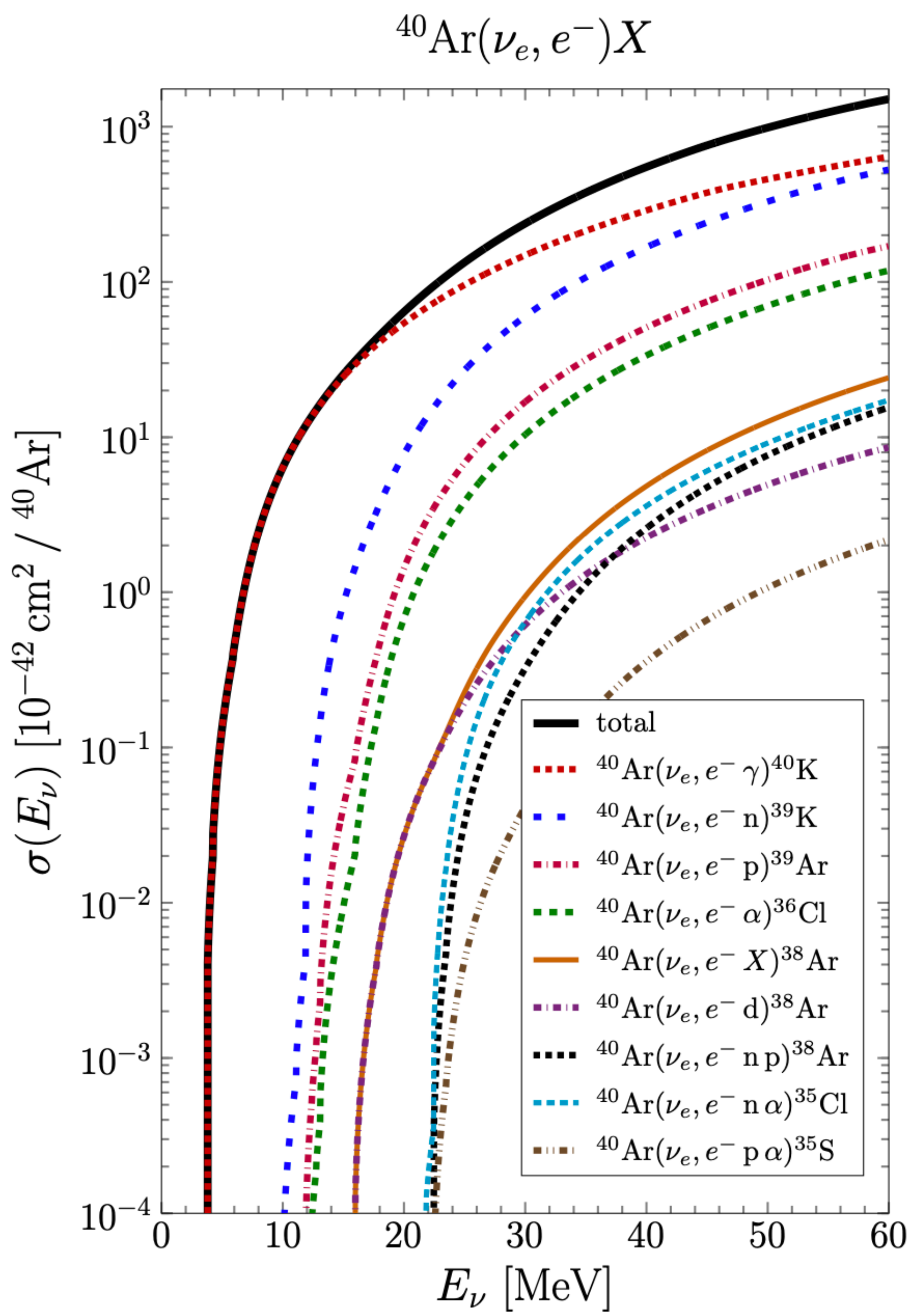

S. Gardiner, Phys. Rev. C 103, 044604 (2021)

I. Inclusive scattering on the nucleus:

Allowed approximation (long–wavelength ($q \to 0$) and slow nucleons ($p_N/m_N \to 0$) limit), Fermi and Gamow-Teller matrix elements:

II. Nuclear de-excitation:

For bound nuclear states, the de-excitation gamma rays are sampled using tables of experimental branching ratios.

For unbound nuclear states, MARLEY simulates the competition between gamma-ray and nuclear fragment emission using the Hauser-Feshbach statistical model.

10s of MeV Inelastic Neutrino-Nucleus Scattering: Uncertainty

■ CRPA and MARLEY

- **Allowed and forbidden transitions**

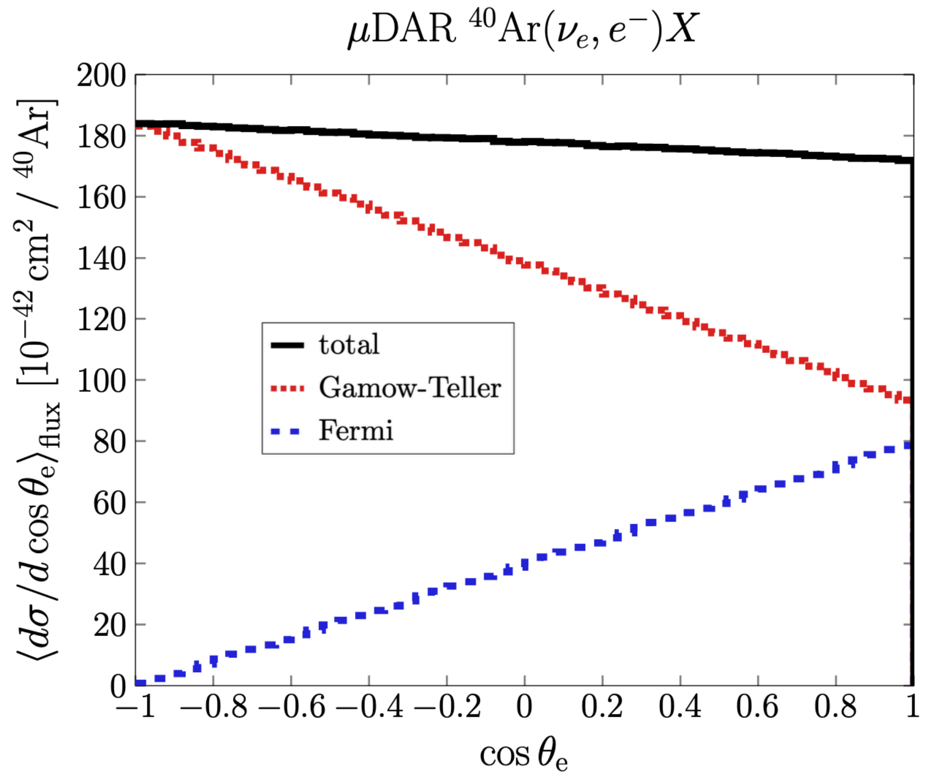

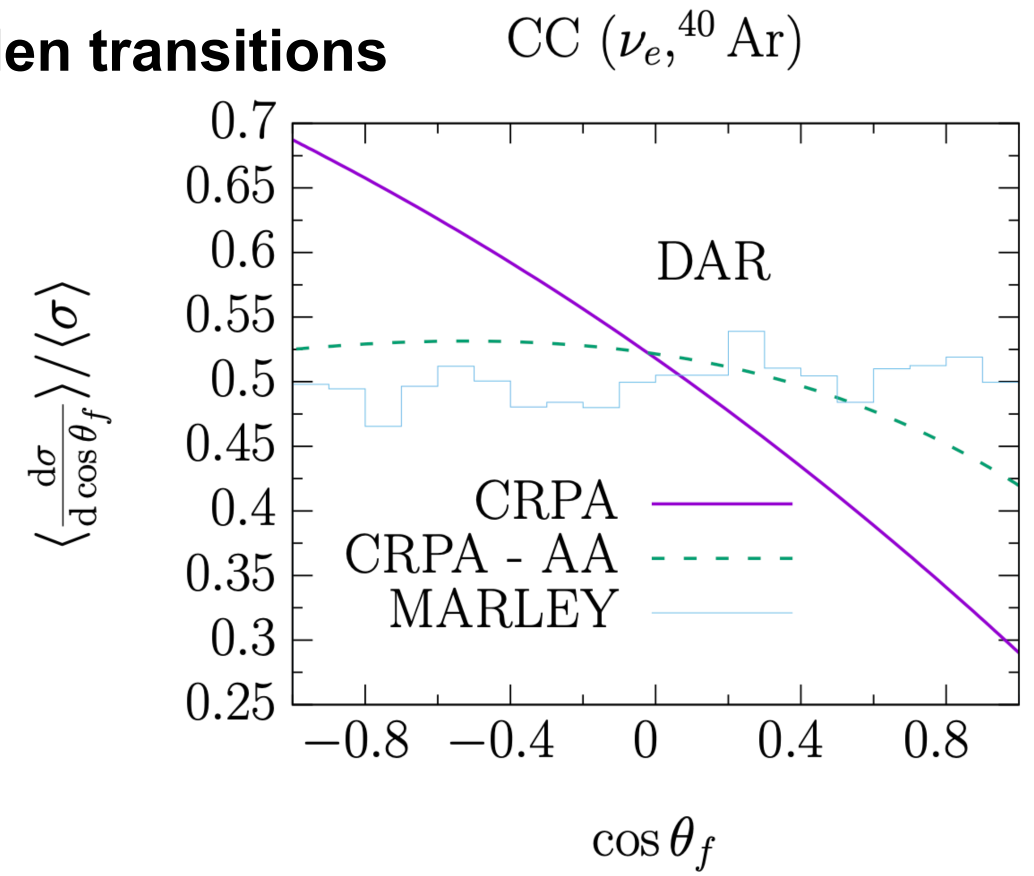

- MARLEY (only allowed transitions, Fermi and Gamow-Teller matrix elements) predicts a nearly flat angular distribution.
- CRPA includes full multipole expansion of nuclear matrix element (allowed as well as forbidden transitions), predict more backwards strength.

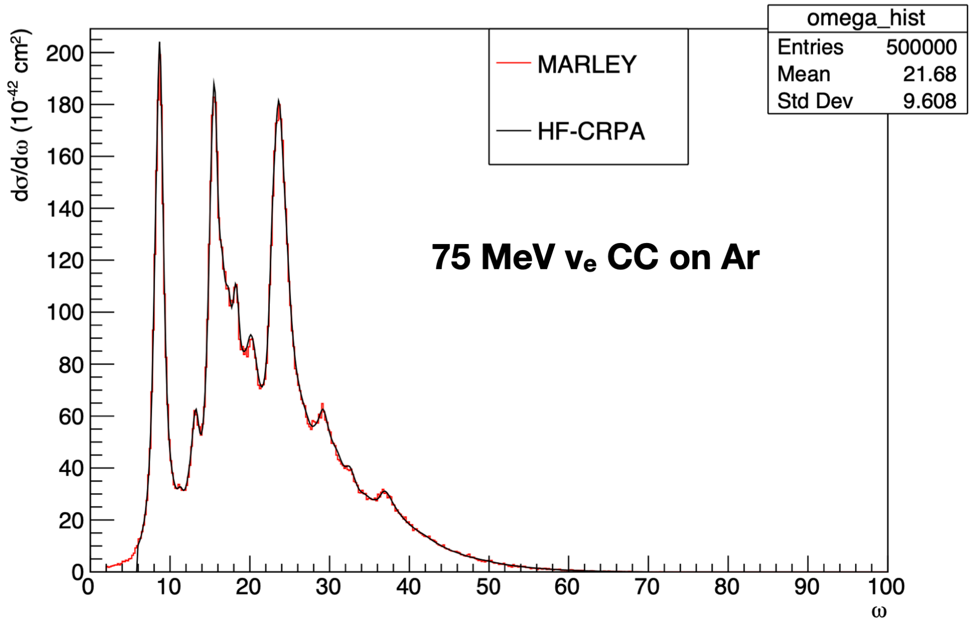

- CRPA implementation in MARLEY is on-going.

(work with Steven Gardiner, Alexis Nikolakopoulos, …)

10s of MeV Inelastic Neutrino-Nucleus Scattering: Uncertainty

✦ **CEvNS experiments at pion-decay at rest facilities - COHERENT at ORNL and CCM at LANL, well suited to perform these measurements.**

- **Coherent CAPTAIN Mills at LANL:** 10 ton LAr detector at Lujan center at LANL. Collected data in 2019, 2021, 2022, and currently is in operation.

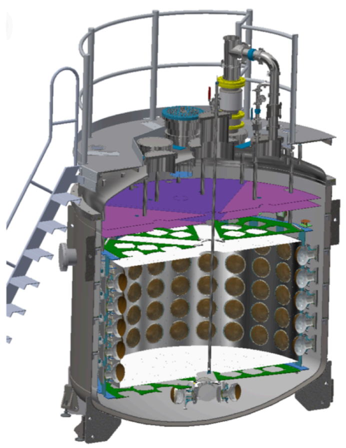

	Total events/year*
CEvNS	300.82
CC (ν_e)	57.25
NC	5.28

*6 months of running, at 23 m, for 5 tons. E_ν =30 MeV.

Preliminary

- **COHERENT at SNS:** COH-Ar-10 (24kg) LAr detector.
  COH-Ar-750 (750 kg) LAr detector is underway.

- **Electron Scattering experiment**

  - MAGIX Collaboration at MESA (Mainz):
  MESA, a new cw multi-turn energy recovery linac for precision particle and nuclear physics experiments with a beam energy range of 100-200 MeV is currently being built.

10s of MeV Physics in GeV-scale Neutrino Beams

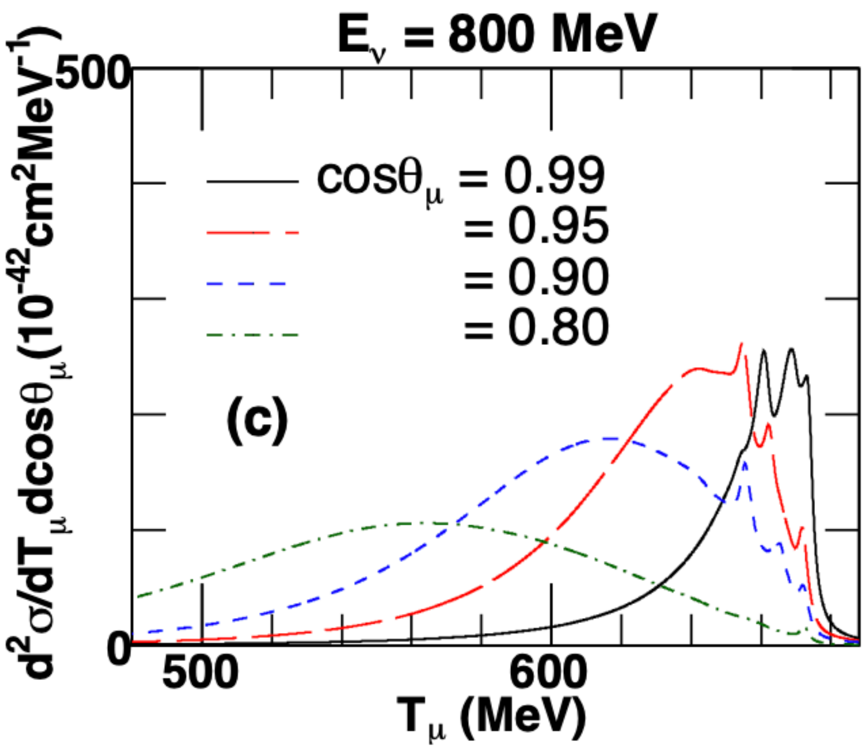

VP, N. Jachowicz, T. Van Cuyck, J. Ryckebusch, M. Martini, Phys. Rev. C92, 024606 (2015)

Folded with BNB ν_μ flux

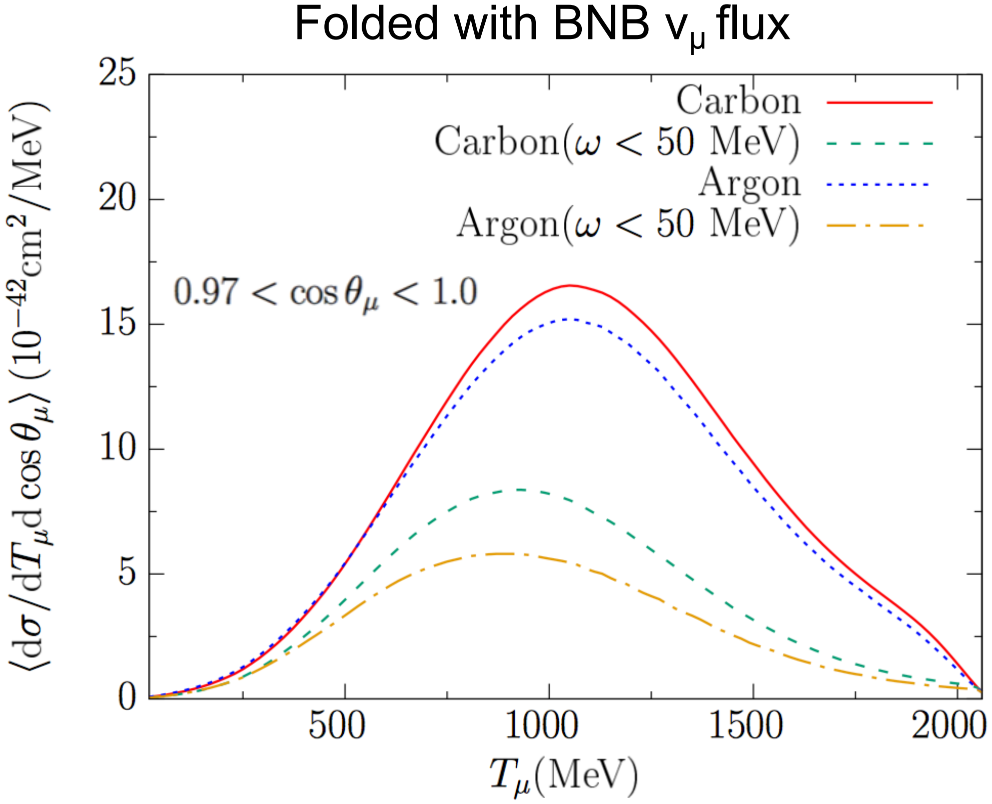

N. Van Dessel, N. Jachowicz, R. González-Jiménez, VP, T. Van Cuyck, Phys. Rev. C97, 044616 (2018).

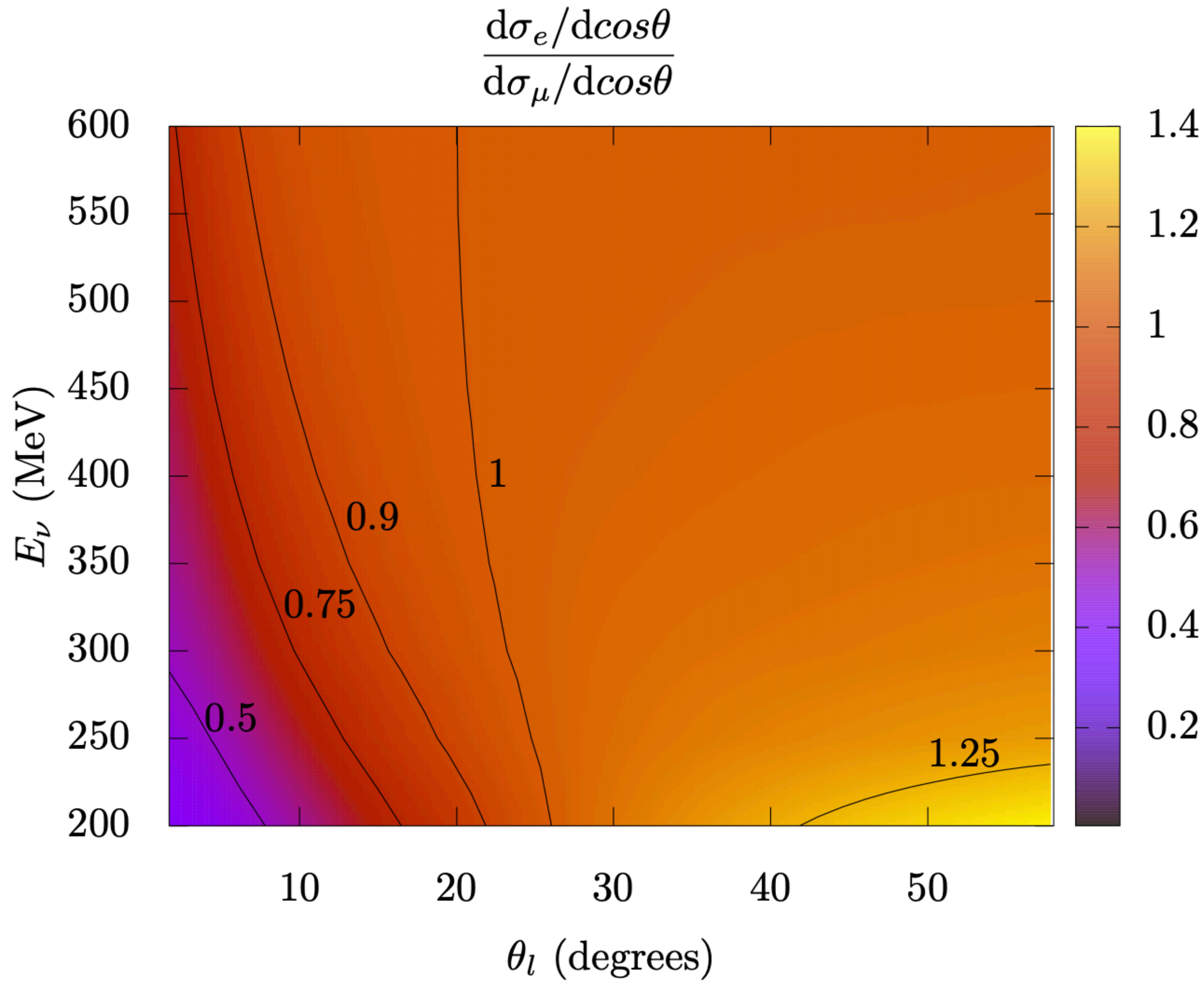

A. Nikolakopoulos, N. Jachowicz, N. Van Dessel, K. Niewczas, R. González-Jiménez, J. M. Udías, VP, Phys. Rev. Lett. 123, 052501 (2019).

- At forward scattering angles (low momentum transfer), the neutrino-nucleus cross section at GeV-scale energies is impacted by the same nuclear physics effects that are important for the low-energy case more generally.
- At these kinematics, differences between final-state lepton masses become vital and affect the ratio of the charged-current ν_e to ν_μ cross sections.

10s of MeV Physics in GeV-scale Neutrino Beams

- Mono-energetic KDAR neutrinos at NuMI beam dump (FNAL) and at MLF (JPARC).

$$K^+ \rightarrow \mu^+ \nu_\mu,\ E_{\nu_\mu} = 236\ MeV$$

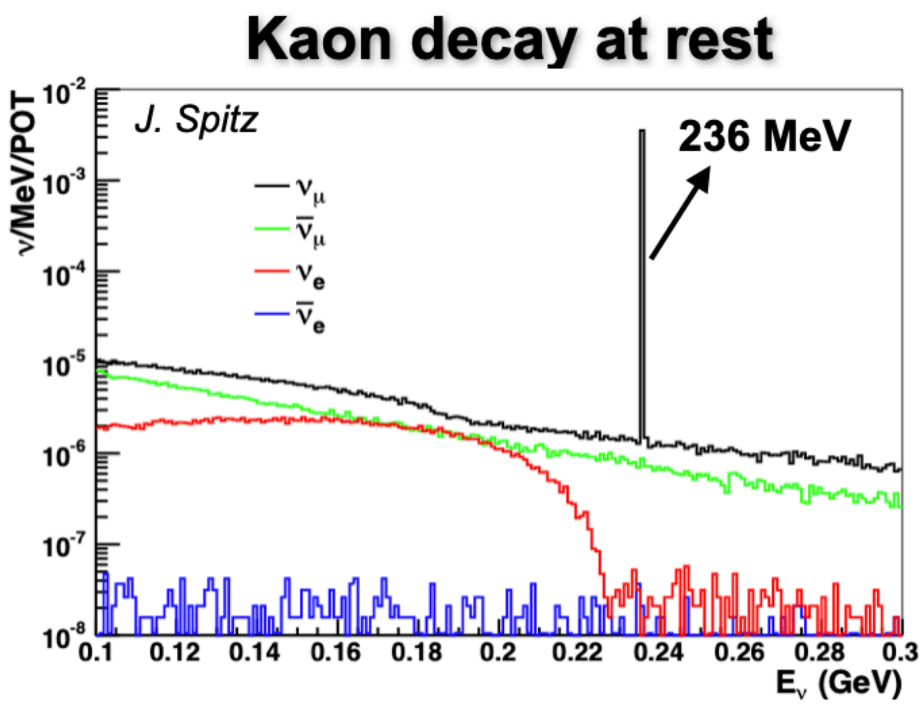

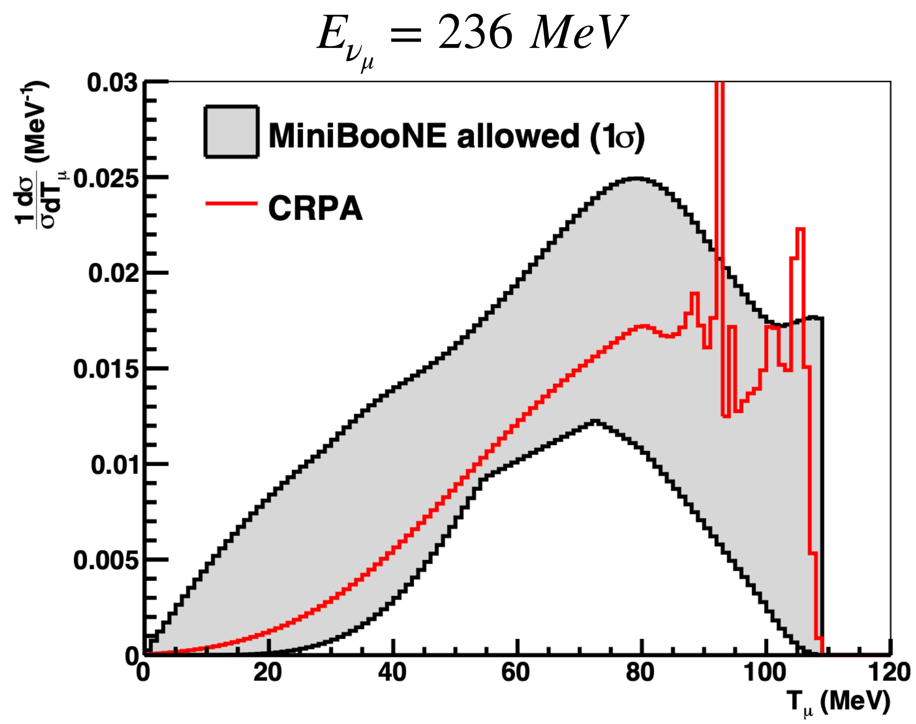

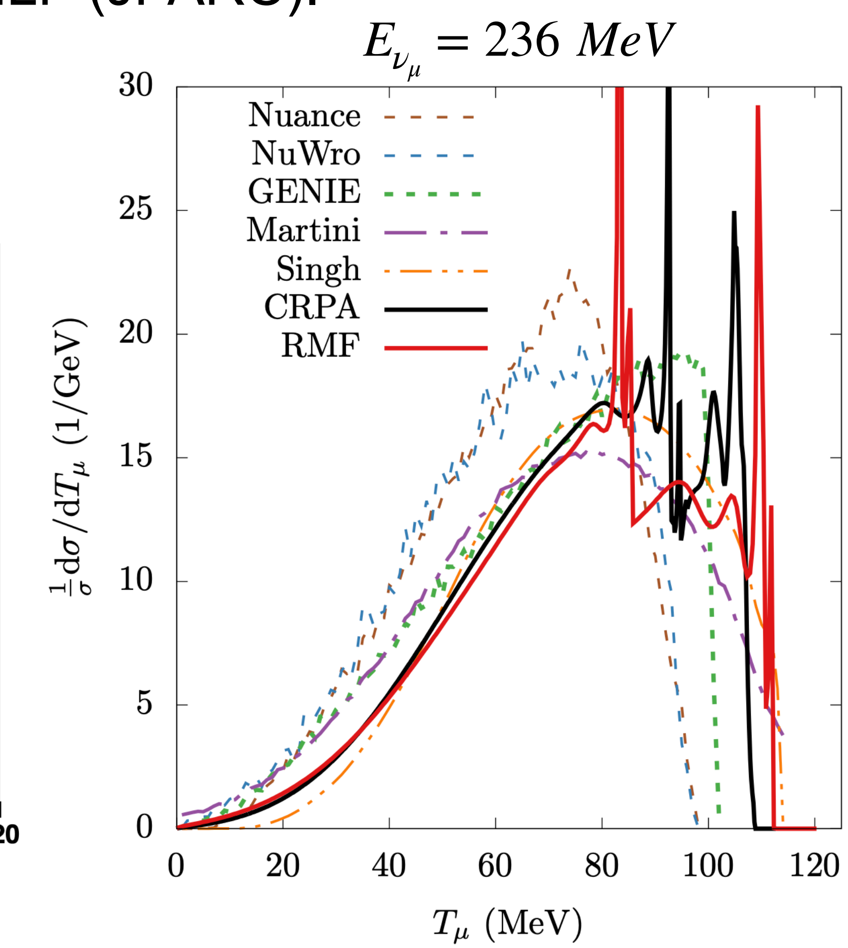

A. Nikolakopoulos, VP, J. Spitz and N. Jachowicz, Phys. Rev. C 103, 064603 (2021)

MiniBooNE data: Phys. Rev. Lett. 120, 141802 (2018)

- Exciting near future measurements: MicroBooNE and ICARUS (argon), JSNS^2 at J-PARC (carbon).
- 240 MeV electron scattering measurement planned at Mainz.
- Combined analysis of mono energetic electron and ν_μ cross sections will give great opportunity to constrains axial response at fixed energy.

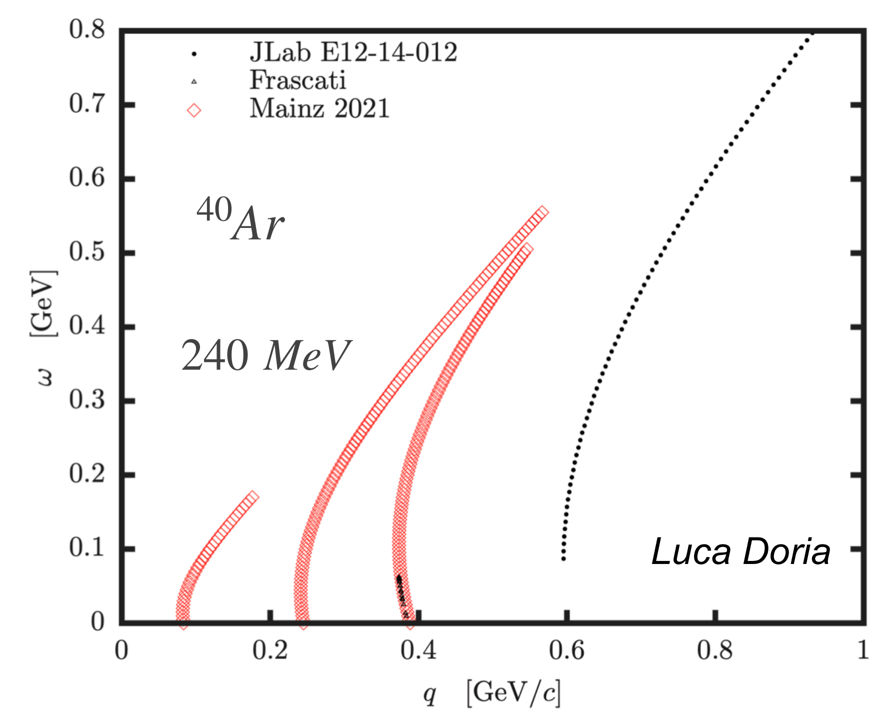

Summary

- Interactions of low energy (10s of MeV) neutrinos - elastic (CEvNS) and inelastic - are interesting for studies of various nuclear, neutrino, BSM and astrophysical processes.

- Neutrino-nucleus interactions at these energies are sensitive to neutron radius and weak elastic form factor (CEvNS), and underlying nuclear structure (inelastic).

- Microscopic calculations, future precise measurements of CEvNS cross section and PVES asymmetry measurements will enable precise determination of weak form factor and neutron distributions.

- CEvNS experiments at stopped-pion sources are powerful avenues to measure 10s of MeV inelastic CC and NC neutrino-nucleus cross sections. These measurements will play a vital role in enhancing DUNE's capability of detecting core-collapse supernovae neutrinos.